A STUDY ON THE AIR TO WATER INTERFACE: CO_2 FLUX RATES FROM UVAS RESERVOIR LOCATED IN A MEDITERRANEAN CLIMATIC REGION

By

JULIANNA PORRAZ

THESIS

Submitted in partial satisfaction of the requirements for the degree of

MASTER OF SCIENCE

in

DEPARTMENT OF CIVIL AND ENVIRONMENTAL ENGINEERING

in the

OFFICE OF GRADUATE STUDIES

of the

UNIVERSITY OF CALIFORNIA

DAVIS

Approved:

Holly J. Oldroyd

Alexander L. Forrest

Fabian Bombardelli

Committee in Charge

2023

ABSTRACT

Freshwater reservoirs are hotspots for methane (CH_4) and carbon dioxide (CO_2) fluxes released into the atmosphere; however, there is little knowledge about CO_2 flux rates from reservoirs in Mediterranean climate regions. Studies show that reservoirs can either emit or absorb CO_2, depending on the season and time of day. The goal of this study was to analyze CO_2 and gain knowledge of the temporal variability of CO_2 fluxes at Uvas Reservoir, Santa Clara County, California, in a Mediterranean climate zone. Results showed a strong diel variability of CO_2, with negative flux rates (CO_2 sinks) generally occurring during the nighttime. For example, in June 2021 at Uvas Reservoir, CO_2 flux rates decreased from -0.27 mg $\cdot$ m^{-2} h^{-1} to -0.48 mg $\cdot$ m^{-2} h^{-1} at night. These fluxes were also variable seasonally, where positive values (CO_2 sources) in CO_2 fluxes occurred during fall turnover, with a peak flux rate calculated at +1.57 mg $\cdot$ m^{-2} h^{-1} in the daytime. This example from the fall season occurred after the reservoir had used up all the nutrients and when algae were decomposing. Lastly, the CO_2 surface gas flux results from Uvas Reservoir were compared to other freshwater reservoirs within the same climatic region, different climatic regions, and other land classification types. This comparative analysis showed that Uvas Reservoir had 20% and 6.2% higher CO_2 flux rates compared to a tropical climate and a temperate climate in a dry year, respectively.

CONTENTS

LIST OF FIGURES

LIST OF TABLES

ACKNOWLEDGEMENTS

I would like to take the time to give credit to where its due and acknowledge the team effort put into the development of this project. This study would not have been done without the help and continued support from:

- My PI's and project supervisors: Dr. Holly J. Oldroyd and Dr. Alexander L. Forrest who provided their assistance, much patience and encouraged my growth throughout my academic career.
- The team of graduate students on this project that put in the endless hours and assistance towards the project: Ruth Thirkill, Wilton Gray IV, Corrin Clemons, and Douglas Kubota.
- The team of undergraduate students who dedicated their time to volunteer for the monthly 24-hour field deployments: Sergio Jimenez, Noah Skelly, Christina Angelos, and Zender Matsumoto (to name a few).
- The Santa Clara Valley Water staff and volunteers: Mark Seelos and Olivia Trevino.
- My dearest family for their constant love and never-ending support x 10.
- L.A.M. for all the love, time, and patience you have given. You continue to inspire me.

To My Beloved Grandmother Who Was My Light.
Thank You.

CHAPTER 1 INTRODUCTION

1.1 Project context

The carbon cycle is a biogeochemical process known for the exchange of carbon across terrestrial, oceanic, and freshwater interfaces within the atmospheric. A component of the carbon cycle is the emission of carbon dioxide (CO_2) released into the atmosphere from inland freshwater ecosystems. CO_2 has an active role in the Earth's energy budget, which is an efficient greenhouse gas (GHG) that traps heat in the atmosphere (Raymond et al. 2013). CO_2 is needed to keep the global surface temperature from freezing (NOAA, 2022). However, with an overabundance of CO_2 from anthropogenic sources, the GHG can contribute to global warming by supercharging the natural GHG effect (Lindsey, 2022). The levels of CO_2 have increased by 61 parts per million (ppm) since 1990 and account for 80% of the increased heating of atmospheric temperatures on a global scale (NOAA, 2022).

Freshwater reservoirs deliver a plethora of benefits for a growing population. For example, they aid in providing flood control, hydropower, water supply, and sustaining biodiversity. Nonetheless, they can have a global role in the production and emission of potent greenhouse gases (GHGs). They contribute to global carbon budgets where dissolved gases like methane (CH_4) and carbon dioxide (CO_2) are transitioned from terrestrial and aquatic carbon to atmospheric biomes as they regulate the transfer of organic carbon to the atmosphere through vertical gradients that drive diffusion (Deshmukh et al. 2014; St. Louis et al. 2000; Pollard, 2022). Nitrous oxide (N_2O) is another dissolved gas that has nearly 300 times the warming power of CO_2 and is also found in freshwater ecosystems (Delsontro et al. 2015).

Although all GHGs act as major generators of climate change, the objective of this thesis will be primarily focused on the carbon cycle where CO_2 is most relevant. This thesis analyzes

three freshwater reservoirs that are owned and operated by Valley Water and located in Santa Clara County in Northwestern California. The collected data are used to calculate the monthly CO_2 water to air fluxes throughout a year range to determine the diel and spatial variability identify if Mediterranean reservoirs are a CO_2 contribution to net carbon sink or net carbon source throughout.

CHAPTER 2 BACKGROUND AND LITERATURE REVIEW

2.1 Lentic Systems

Freshwater reservoirs are lentic systems and have smaller surface areas compared to coastal waters, yet have a significant role in regulating carbon fluxes (Kosten et al. 2010). There are significant physiochemical and biological activity within these freshwater ecosystems that enhance the transport of CO_2 fluxes across the both the sediment and atmosphere boundary. For example, dissolved CO_2 gas flux rates are appreciably higher in smaller lakes due to the occurrence of surface layer cooling, mixing and turnover in most stratified water bodies. (Macintyre et al. 2002). Exploration of the pre-turnover and post turnover periods in reservoirs will further encapsulate the seasonal and diurnal timescale of CO_2 and identify if CO_2 highest emission rates ("hotspots") are solely dependent on the seasonal stratification period. The geomorphic location, longitudinal and latitudinal location of the reservoir are equally as important, as certain climatic zones may experience distinctive and variable meteorological and water quality conditions (Brown et al. 2020).

Globally, there are six major climate classifications: polar, temperate, arid, tropical, Mediterranean, and mountainous regions. The geographic coordinate system remains as a reminder of how environmental systems play a role on the flux emissions from reservoirs. These factors can impact the biogeochemical conditions and depending on the season, may also impact the desiccated or dried out areas. Evidently, various hydrological dynamic environments (i.e., stochastic desiccation or water fluctuation periods at reservoirs) are often not included into carbon budgets which may have misleading and underestimated budget calculations (Keller et al. 2020). The significance of this study lies particularly on understanding and mitigating climate change impacts where both water and nutrient cycling have been altered as a result of ecosystem

shift due to warming climate conditions (Deemer et al. 2016). It is critical for water managers to reach carbon neutrality and consider these bodies of water in quantitative carbon models (Cole et al. 2007).

2.2 Mediterranean Reservoirs

The location, morphology and certain atmospheric conditions of an artificial lake will affect the surface water concentrations of CO_2 (Wetzel, 2001). The Mediterranean climate or dry-summer climate (Cs) is a major climate group based on the Köppen climate classification. It is commonly associated with hot, dry summers and cool, rainy winters (Lionello et al. 2012). This climatic region is primarily located between 30 and 40 degrees north and south of the equator, on the western coasts of continents. The Mediterranean climate has an average temperature above 0°C (32°F) and below 18° C (64°F) in the coolest months (Lionello et al. 2012). There are two major seasons in Mediterranean climates: summer and winter where the seasonal changes are a result from nearby ocean currents and ocean water temperature. The summer and winter seasons experience considerable atmospheric phenomena patterns. Throughout the summer in coastal areas (e.g., California), the cold currents often cause thick layers of marine fog that usually clears by mid-day but occurs from the stabilizing effects on the surrounding air. There is a noticeable diel character to the daily temperatures in the warm summer months due to thermal heating during the day and rapid cooling at night. Valley Water's operated and managed reservoirs are in the northwestern Mediterranean coast of the United States in Santa Clara County, which is subjected to hot and arid conditions in the summer yet has the potential to experience cold and wet winters. During La Niña, the pacific jet stream meanders into the North Pacific resulting in warmer and dryer weather atmospheric conditions (Lindsey, 2017). Whereas During El Niño, the opposite occurs and there are cooler and wetter atmospheric conditions (Lindsey, 2017).

2.3 Sedimentation

Carbon is usually stored in bottom sediments of a reservoir. Sediments have had a unique reaction with the changing climate as reservoirs have desiccated (Keller et al. 2020). During desiccation periods, sediments are exposed to the atmosphere and have shown to release a larger amount of carbon dioxide effluxes than when inundated (Keller et al. 2020). As the reservoir's water is reconditioned, atmospheric conditions like wind and rain will have an impact on the CO_2 flux rates. Moreover, resuspended sediments are prone to wind-induced motion acting on the sediments (Keller et al. 2020; MacIntyre and Melack 1995). This is due to the condition of the sediment and the effects of the water currents.

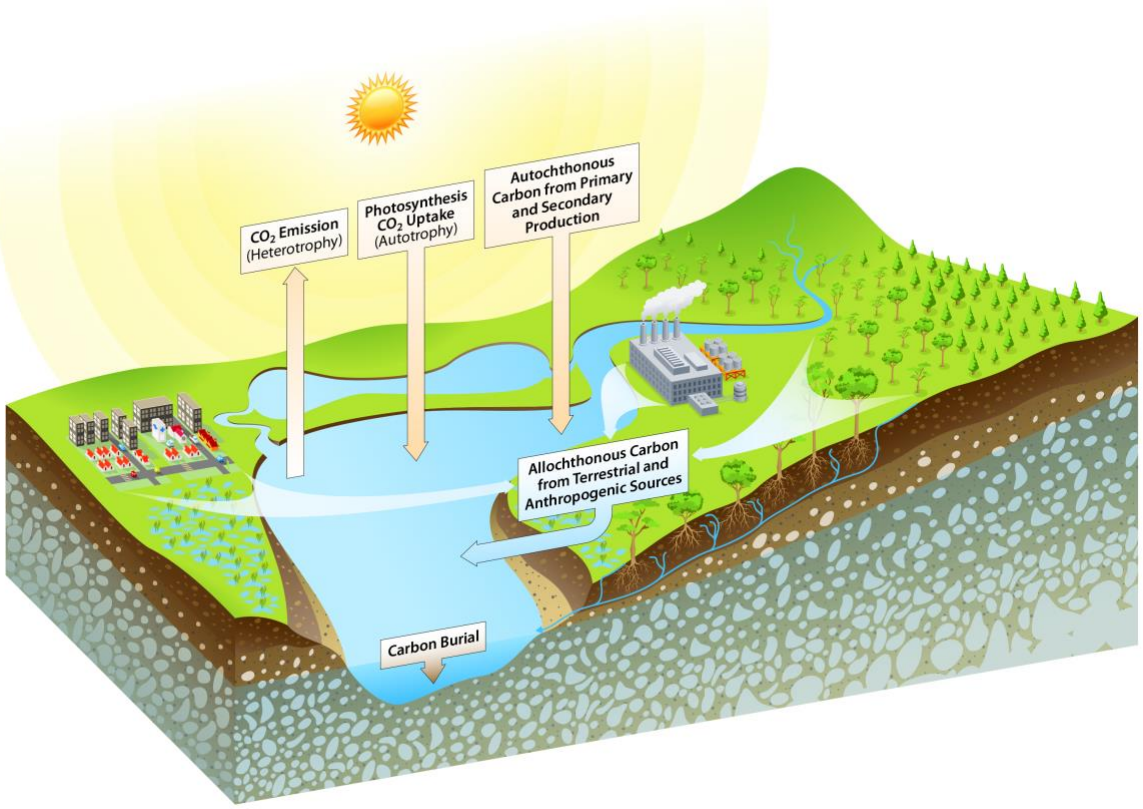

Figure 2.3.1 CO_2 modes of flux pathways in aquatic environments. Schematic taken from Butman et al. (2018).

Generally, aquatic ecosystems are found to produce larger amounts of sedimentation, and the input of allochthonous organic matter events are more prevalent (Montes-Pérez et al. 2022). Inland waters are representative of both natural and anthropogenic influences of carbon flow (*Figure 2.3.1)* (Butman et al. 2018). Under anoxic condition, when the water is deprived of oxygen, and when the reservoir is stratified, allochthonous organic carbon mineralization is suppressed leading carbon to sink within the sediments (Tranvik et al. 2009; Eugster et al. 2003). Under extreme weather (i.e., a major storm event), there is an increase in suspended sediments, causing the CO_2 to be supersaturated, which results in the surface water becoming a source of CO_2 (Park and Chung, 2018).

2.4 Inorganic Carbon Complex

Dissolved inorganic carbon (DIC) is responsible for the foundation of organic productivity and the influence of gaseous and nutrient availability characteristics (Wetzel, 2001). In comparison to any other gases, the behavior of CO_2 in water is complex by the chemical reactions of hydration reactions (Smith, 1985). When the reservoir absorbs the elevated CO_2 from the atmosphere, carbonic acid (H_2CO_3) forms which is then deprotonated rapidly, forming bicarbonate (HCO_3^-) which is responsible for releasing hydrogen ions - decreasing pH (water becomes more acidic) (Horne and Goldman, 1994; Brown et al. 2020). This is because of the chemical reactions of hydration of carbonic acid to bicarbonate and carbonate (*Equation 1)* (Smith, 1985).

$$CO_2\ (air) \rightleftharpoons CO_2(dissolved) + H_2O \qquad \text{(Equation 1)}$$

at a half-time of approximately 15s, the dissolved CO_2 hydrates by a slow reaction.

$$CO_2 + H_2O \rightleftharpoons H_2CO_3 \qquad \text{(Equation 2)}$$

at a low pH of less than 8 the reaction given by (*Equation 2)* predominates with 0.25% of the dehydrated CO_2 at the equilibrium concentration of H_2CO_3 (Wetzel, 2001).

The DIC is dependent on the different factors that influence its concentration, for instance, lake size, age, and lake productivity (Brown et al. 2020). Nonetheless, DIC has a dependent relationship on the pH of the water which is largely influenced by the buffering capacity of the carbonic acid and bicarbonate and carbonate reactions (Wetzel, 2001). The increase in DIC and a decrease of pH has a negative long-term effect on organisms and freshwater biota by acidifying the water column (Brown et al. 2020). However, some freshwater systems have notable seasonal or localized DIC limitations (Brown et al. 2020).

2.5 Seasonal CO_2 Observations from Previous Literature

Monomictic lakes mix from top to bottom once each year (*Figure 2.5.1)*. Starting with the winter season, the lake is less productive and the surface and deep-water temperatures become isothermal post fall turnover. The dissolved oxygen (DO) in the water is limited by the lack of photosynthetic processes taking place. The nutrients remain in the sediment bed from the internal loading; however, the nutrients are also introduced into the lake through external loading like runoff. In the spring, the lake experiences warming atmospheric temperatures and the surface water becomes warmer from the direct sunlight during the daytime. Stratification begins to take place in the water column from early spring all throughout summer when the temperature of the water is warming up. Most of the nutrients began to be used up by the aquatic biota and phytoplankton during warmer water temperatures. Spring is prime time for the water body to

experience high uptake of CO_2. Meanwhile, the DO is released through photosynthesis and through normal respiratory scenarios. When it finally reaches the summer months, the lake has already passed its peak productivity time and the remaining nutrients will be consumed by the biota. This scenario acts as a Mobius loop, a feedback mechanism which is indicative of phytoplankton using the free CO_2 for photosynthetic processes. However, due to high concentration of plant biota and organisms, there are also phytoplankton that do not have access to the sustaining resources like light and CO_2 and thus, begin to die off (Casper et al. 2000). There remain questions about whether the summer months identify as a sink or source of CO_2. In the fall, destratification occurs, mixing takes place, and the DO is reintroduced into the lake from the free atmosphere. Meanwhile, all the nutrients have been consumed and the water body is supersaturated with CO_2 causing the body to act as a net source.

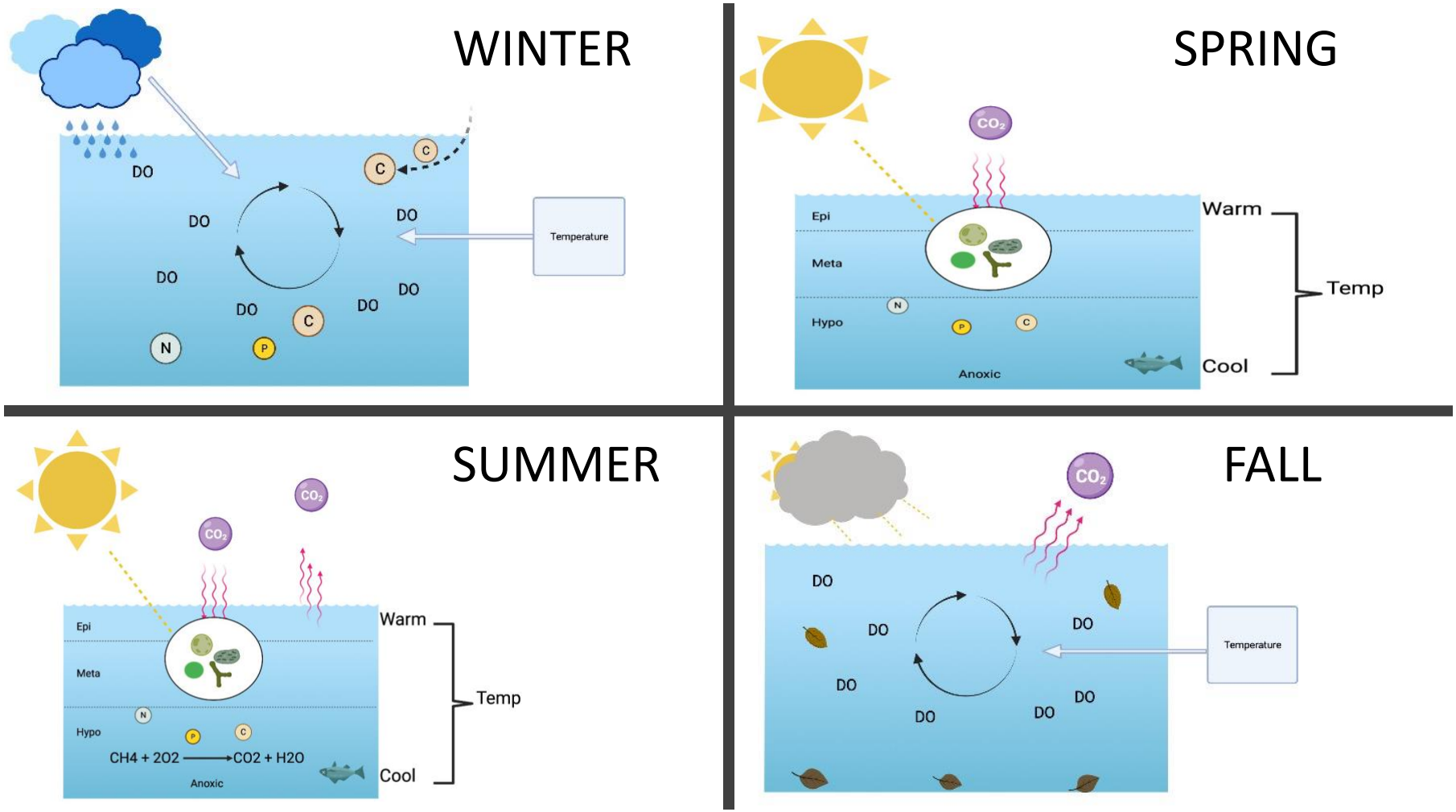

Figure 2.5.1 Seasonal responses in reservoir based off (Fafard, 2018). In the winter season, the reservoir can either act as a CO_2 source or a sink depending on the trophic state of the water body (Arrows represent the winter runoff and the reloading of C). In the spring season, the reservoir is ready for prime uptake for CO_2. In the summer season, the nutrients are limited and can be a large sink but also the algae are dying off thus causing an efflux of CO_2. In the fall season, the reservoir undergoes destratification and will mix to redistribute DO and organisms into the water column.

2.6 Magnitude of CO_2 Exchange Determined by Partial Pressure

CO_2 is exchanged into the atmosphere when the surface of the freshwater reservoir reaches complete saturation. The partial pressure of CO_2 (P_{CO2}) is a main driver of CO_2 flux, when the P_{CO2} in the water is greater than in the atmosphere (Park and Chung, 2018). Aquatic P_{CO2} levels are a result of both external and internal processes that are driven by the interplay of thermodynamic effects, physical mixing, and biological activities at different time scales (López et al. 2011). Calculating the maximum concentration of the air balanced with the water can be found using Henry's law (*Equations 3-6*).

$$CO_2 + H_2O = CO_2\ (aq) \qquad K_{HCO_2} = 0.031 \frac{M}{atm} \qquad \text{(Equation 3)}$$

where the molar mass of CO_2 is 44.01 g per 1 mol, and the solubility of CO_2 in water at 25°C is 1.7 mg/L. This simplifies to $2.5 * 10^4 \frac{L}{mol}$ however we want in units of $\frac{mol}{L}$.

$$44.01 \frac{g\ CO_2}{1\ mol\ CO_2} * \frac{1000\ mg}{g} * \frac{1\ L}{1.7\ mg} = 2.5 * 10^4 \frac{L}{mol} \qquad \text{(Equation 4)}$$

the reciprocal of *equation 4* yields units of molarity.

$$[CO_2] = \frac{1}{2.5*10^4} \frac{L}{mol} = 3.9 * 10^{-5}\ M \qquad \text{(Equation 5)}$$

the partial pressure of CO_2 is found by dividing the concentration of CO_2 from Henry's law constant (*Equation 5* divided by *Equation 3*) to yield:

$$P_{CO2} = \frac{[CO_2]}{K_{HCO_2}} = \frac{3.9*10^{-5}\,M}{0.031\frac{M}{atm}} = 1.25 * 10^{-3} atm * 10^6 \qquad \text{(Equation 6)}$$

multiplied by 10^6 where one part per million (ppm) denotes one part per 10^6 to give the maximum concentration of the air balanced with water.

$$P_{CO2} = 1.25 * 10^3\ ppm \qquad \text{(Equation 7)}$$

Where Henry's law constant $K_{HCO_2}\ is\ 0.031\ \frac{M}{atm}$ for CO_2 gas in water at 25°C. The calculations above show that under ideal temperature conditions, the P_{CO2} is in balance with the atmosphere at $1.25 * 10^3\ ppm\ or\ 1.25 * 10^3\ moles\ of\ CO_2\ in\ a\ million\ moles\ of\ air$ *Equation 7* and will become supersaturated if it increases.

In summary, the cooling of a reservoir results in an increase of P_{CO2} (Czikowsky et al. 2018). P_{CO2} tells of the physical conditions of the water and is a critical component for analyzing the transport of CO_2 flux (F_{CO2}) to the atmosphere. Most reservoirs experience supersaturation and result in autotrophic conditions where CO_2 is being produced at a faster rate than it is consumed, thus resulting in an output of F_{CO2} (Cole et al. 1994). Supersaturation is when the P_{CO2} in the atmosphere is less than the P_{CO2} in the water. When supersaturation occurs in the water column, it releases concentrations of CO_2 into the atmosphere. However, when the water column is undersaturated there is an absorption of CO_2 instead (Park et al. 2021). Generally, from the variation in CO_2 saturation caused by the physical conditions of the water, reservoirs can act as either sink or a source for CO_2 (Cole et al. 1994; McDowell, 2017).

Additionally, in a Mediterranean climate, CO_2 effluxes transpire on a seasonal scale during the turnover period that extends from spring to fall (Montes-Pérez, Marcé, et al. 2022). When

destratification occurs, the accumulated gas stored in the hypolimnion is ventilated upward and diffused through vertical mixing into the atmosphere. When P_{CO2} is supersaturated, and the surface water is in equilibrium with the atmosphere the reservoir will expel large pulse emissions of CO_2 during the turnover period (Park and Chung, 2018). Overall, thermal stratification and mixing processes are drivers of CO_2 pulse emissions namely in stratified reservoirs (Liu et al. 2016; Park and Chung 2018).

2.7 Air-water exchange mechanisms

A very important environmental process is the transfer of substances between air and water (Mackay and Shiu, 1984; Brutsaert and Jirka 2013). There are diffusive and non-diffusive pathways which are both equally important modes of transporting and regulating gas exchange between the air-water interface. Diffusion and ebullition are the two most significant pathways of GHG emission. Where CO_2 and N_2O are soluble in water (diffusion is the prime pathway), CH_4 is mostly insoluble in water (both ebullition and diffusion are pathways) (Deemer et al. 2016). The Henry's Law constant which characterizes the air-water equilibria, is used to partition the coefficient, and directly quantify the direction and rate of transfer of the gas. Current methods for quantifying gas transfer are based on CO_2 diffusive flux emissions.

2.7.1 Diffusive exchange

The most common gas transfer pathway from the water interface to the air is through diffusion. CO_2 is primarily diffused through the mass boundary layer due to its low solubility in water (McGinnis et al. 2015; Vachon et al. 2010). Thus, gas fluxes are estimated through diffusive methods and are useful for quantifying F_{CO2} from reservoir surfaces. Namely, diffusive processes are driven by the fugacity or difference in chemical potential of the chemical between the air and water (Mackay and Shiu, 1984). Due to the nature of CO_2 in water, high

concentrations can accumulate and thus diffuse at shallow depths due to its high solubility (Casper et al. 2000). More specifically, diffusion of CO_2 diffuses slowly but can be accelerated by turbulent mixing which can occur in the epilimnion of the lake (Horne and Goldman 1994).

2.7.2 Ebullitive exchange

Gases can be emitted from surface waters to the atmosphere through ebullition also known as bubble transfer. In this type of pathway, the hydrostatic pressure is formed when water becomes more hydrophobic for methane in the sediments and due to the hydrophobicity, the bubbles end up at the surface of the water (Graziano, 2014). This process is highly variable in space and time. The ebullitive exchange responds to the increase of water levels, where the hydrostatic pressure increases in the wet winters and decreases in the dry summers leading to low emissions and high emissions, respectively (Bastviken et al. 2004). Ebullitive fluxes are evident through sightings of spontaneous bubbles at the water surface largely seen in the summer months. Out of all the other gases, this is a notable dominant pathway for CH_4 as it is less soluble in water. The role that these bubbles play in contributing to CO_2 concentrations is through a mechanism called methane stripping. This occurs when CH_4 becomes oxidized in the mixed layer and converts into CO_2 (Tranvik et al. 2009).

2.7.3 Monitoring diffusive flux emissions

In comparison to diffusive fluxes, ebullitive fluxes are found to be minimal and the most dominant flux pathway for CO_2 is through surface diffusion (Bevelhimer et al. 2016; Deemer et al. 2016). The methods that are used in current studies for determining diffusive fluxes of CO_2 include the thin boundary layer (TBL), the floating chamber (FC) and the Eddy Covariance (EC).

The prime goal of the TBL method (*Equation 8*) is to determine the deficit in the concentration of gas between the air equilibrium to water phase over large areas and a long time

series to quantify the gas flux (Huang et al. 2022). The gas flux of CO_2 is stimulated by Fick's law and is quantified as follows:

$$J = K_L(C_w - sC_a) \quad \text{(Equation 8)}$$

where J is the water to atmosphere positive net flux, C_w is the concentration of the water, s is the solubility coefficient, C_a is the concentration of the air equilibrium and K_L is the CO_2 gas transfer coefficient. K_L is representative of the processes that drive the turbulence-mediated gas transfer across the surface aqueous mass boundary layer (Zappa et al. 2007). A sample of water is injected into a sealed tight container, followed up with forceful mixing for ~2 min to fully equilibrate the gas which is later used to identify both the concentration of CO_2 and the PCO_2. The GHG flux can be calculated from the concentration gradient and the physical transfer coefficient (Huang et al. 2022). From previous studies, it is understood that gas fluxes are perceivably controlled by the concentration gradient between the water and the gas exchange coefficient (Jonathan J. Cole and Caraco, 1998).

The FC method (*Equation 9*) is used to quantify the accumulation of gas flux by placing chambers with a known volume and area on the surface of the water and taking concentration measurements over an allotted time. Generally, quantifying the gas flux using the FC method is given by:

$$J = \frac{\Delta c}{\Delta t} \quad \text{(Equation 9)}$$

J is the flux, Δc is representative of the change of gas concentration and Δt is representative of the change of time over which that change in concentration occurs. The FC is a viable way to measure the flux rates from reservoirs, however; spatial variability is constricted. The FC method can be easily duplicated because of its the ease of construction and generally cheap material(s).

The Eddy Covariance (EC) method introduces a method for upscaling the diurnal and seasonal flux emissions though the installment of an EC flux station at the reservoir study site (Waldo et al. 2021). The EC technique obtains high frequency velocity and concentration data. (Podgrajsek et al. 2014). The EC instrumentation includes a sonic anemometer for three-dimensional wind components and a sonic temperature, and gas analyzers for CO_2 and water vapor measurements. The turbulent energy and CO_2 fluxes in the vertical direction above the lake surface can be derived from the covariances of vertical wind speed (w) and CO_2 concentration (c) (Equation *10)*

$$J_c = \overline{w'c'}. \qquad \text{(Equation 10)}$$

where J_c is the vertical turbulent flux of entity c, the overbar represents a temporal average, and the primes represent the instantaneous turbulent fluctuations relative to the temporal mean (Eugster et al. 2003). The EC method is considerably different compared to the other methods of measuring gas fluxes. It requires robust post-processing, requires meteorological and atmospheric parameters, and provides an integrated gas flux over an upstream footprint of 250-3000 m radius (Chu et al. 2021).

2.8 Research objectives

With altering climatic factors such as warming conditions, less precipitation, less snowpack, and increased drought, ecosystems are undergoing change. The direct implication that climate change has on reservoirs could result in a negative feedback loop. This could be the case when reservoir water dissipates due to dry weather conditions driving large effluxes of CO_2 to be emitted in the atmosphere. The loop continues with the warming conditions from the GHGs and once again large effluxes until a critical event happens.

Conclusively, reservoirs are significant freshwater ecosystems that play a generous role in providing services for a growing population and thus it is critical to maintain and manage regional freshwater. The state of California faces immense challenges with both water availability and water management. The goal of the project is to answer the driving questions which are summarized below.

- How do the natural turnover cycles that occur in Mediterranean reservoirs influence CO_2 flux?
- What are the primary mechanisms that drive the spatial and temporal variability of CO_2 emissions in Mediterranean reservoirs?
- How do the calculated CO_2 flux rates from Uvas Reservoir compare to different climatic regions and land classification types?

CHAPTER 3 METHODOLOGY

3.1 Project Introduction

The collaborative study conducted by both UC Davis and Santa Clara County Valley Water personnel started in February 2021 to investigate CO_2 flux rates from Santa Clara County's owned and operated Mediterranean climate reservoirs (*Figure 3.1.1).*

3.1.1 Period of Study

Field sampling deployments were split into two distinct sampling types, 24-hour sampling events that occurred once a month and quarterly events that occurred once every season throughout the year. All monthly 24-hour field sampling for this study ensued from February 2021 through February 2022 to collect diel and seasonal CO_2 GHG flux rates from Uvas reservoir. An additional two other sites, Chesbro and Stevens Creek reservoir, were included in the study along with Uvas for the quarterly field deployment periods. The quarterly field sampling events were scheduled once per season to further investigate and compare the spatial variability between the carbon storage and gas fluxes at each reservoir. Additional details regarding the two types of sampling events are provided in Sections 3.2 and 3.3.

Additionally, the ancillary variables mentioned in the previous section above were recorded for both sampling deployment types to gain a comprehensive understanding of the environmental and meteorological parameters. Studying the relevant parameters is significant for gaining a full picture and understanding of the drivers of diffusive CO_2 flux respective to the water body location, size, and trophic status.

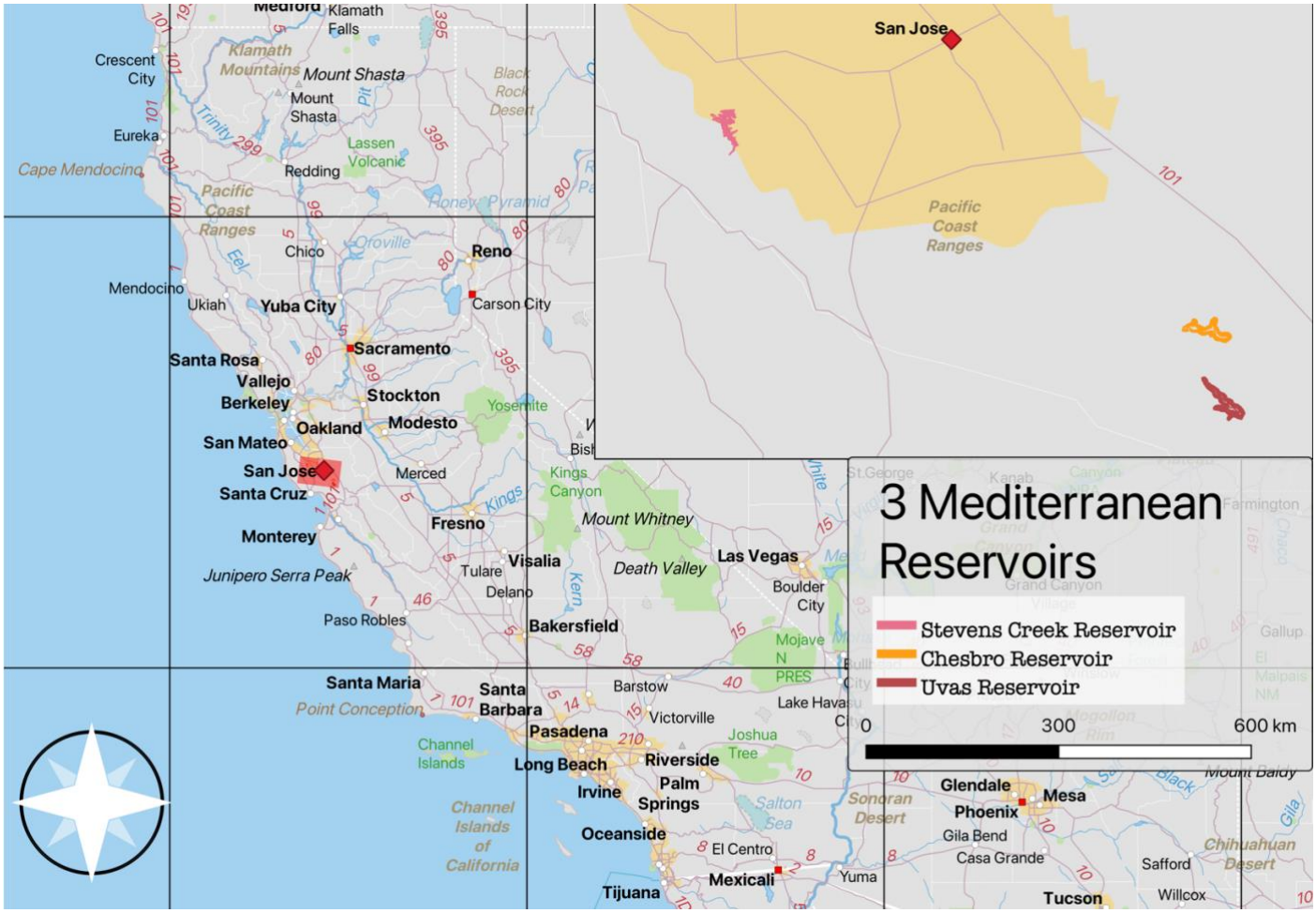

Figure 3.1.1 Map of the three field sites in Santa Clara County: Uvas Reservoir, Chesbro Reservoir, and Stevens Creek Reservoir indicated in the inset by color.

3.2 Monthly 24-hour Field Deployments at Uvas Reservoir

Uvas reservoir was sampled once a month over a time span of 24-hours. During the monthly 24-hour sampling periods, diffusion driven CO_2 surface concentrations, in situ water quality measurements, in and situ meteorological data were collected.

3.2.1 Diffusive Flux Chambers

Floating diffusive flux chambers were constructed by the UC Davis team to be connected to the gas analyzer's inlet and outlet for concentration readings (*Figure 3.2.1.1*). Each diffusive chamber consisted of a 2-gallon bucket (0.00891m^3 volume; 0.0423m^2 cross-section of opening), sampling tube (1/4" OD 1/16" ID), (2) two-way quick connect valves (SharkBite, Cullman, Alabama, USA), a Styrofoam float, aluminum foil and zip ties. The chambers performed as a closed system, with one sampling tube placed through the top of the chamber to pull air from the chamber to the gas analyzer's inlet and then another tube roughly halfway down the side of the bucket that recycled the air from the gas analyzer's outlet back into the chamber.

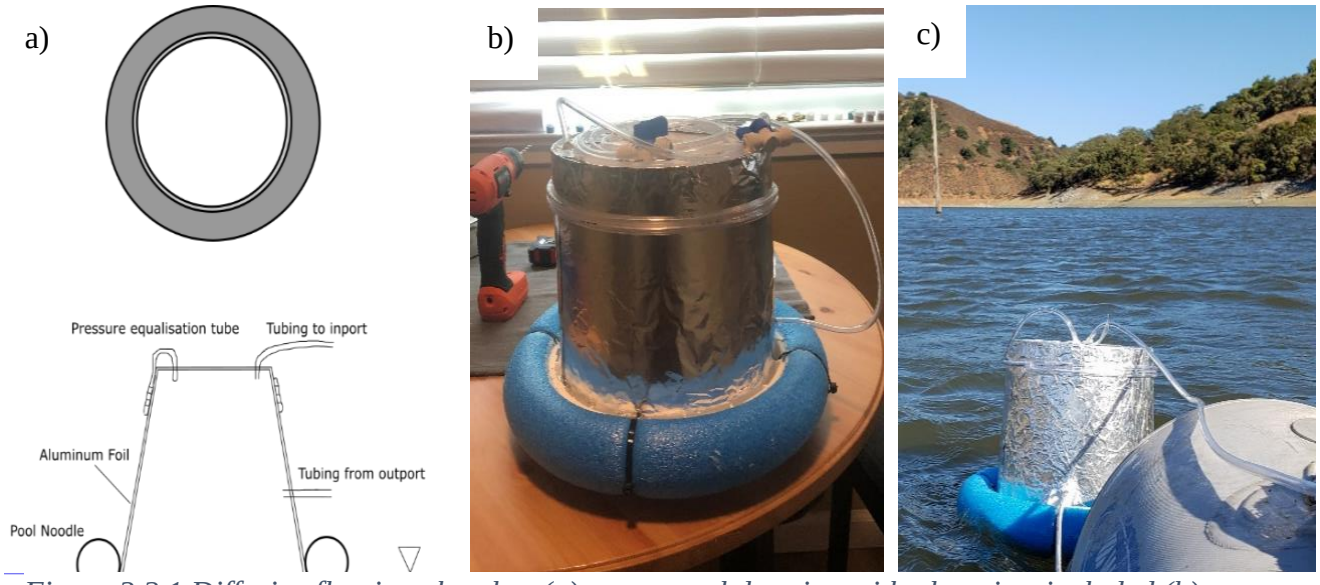

Figure 3.2.1 Diffusive floating chamber (a) conceptual drawing with plan view included (b) constructed diffusive floating chamber, and (c) diffusive floating chamber deployed in the field on Chesbro Reservoir.

Both sampling tubes were connected to two-way valves attached at the end to prevent gas from leaking out when not connected to the gas analyzer. A hole was drilled at the top of the bucket for the tubing to be placed through and then coiled around the side of the bucket to act as a pressure equalizer with the atmosphere (Zhao et al. 2015). Each hole drilled in the bucket was then epoxied on both the inside and outside to ensure a gas-tight seal. The outside of the chamber was then wrapped with aluminum foil to mitigate temperature fluctuations within the chamber due to solar loading. A Styrofoam float was wrapped around the open end of the bucket and secured by waterproof caulking and zip ties. A total of three diffusive flux chambers were created for the project and were each labeled individually for triplicate sampling over the duration of the sampling period(s).

3.2.2 In Situ measurements of CO_2 surface fluxes

Measurements of surface CO_2 concentrations were taken using a greenhouse gas analyzer model ABB LGR-ICOS micro-portable Gas Analyzer 918 (*Figure 3.2.1.2*). The gas measurements are based on laser-absorption spectroscopy. The measurements of CO_2 surface gas concentrations are in parts per million (ppm).

Figure 3.2.2 The LGR gas analyzer that we used for measuring the diffusive flux sample for the study.

A Zodiac boat is used to access each sampling location dependent on the type of deployment (e.g., 24-hour or quarterly) (*Figure 3.3.4b*). The diffusive sampling in the field started by switching on the gas analyzer and making sure the field laptop (Dell Latitude 14 Rugged 5414) connected to the gas analyzer. The VNC Viewer application is software used to access and view real-time data on the field laptop for monitoring the sampling concentrations given in ppm. Data are stored separately

on the gas analyzer's internal storage and can be downloaded later. Next, the three diffusive chambers were deployed on the reservoir water surface alongside the zodiac (*Figure 3.2.1.1c*). The time was recorded for each chamber placed on the water surface and an atmospheric reading along with the time was taken from the gas analyzer for CO_2 concentrations in the atmosphere. The CO_2 concentration and time were recorded after attaching the gas analyzer to Chamber A, and waiting five minutes from the time that the chambers were initially deployed. To get a concentration reading after 5 minutes, the Chamber must be connected to the gas analyzer roughly one minute before the sample concentration is recorded. The total time of a minute and a half is allowed in between samples of chambers A and B, and chambers B and C. This gives enough time to disconnect from the previously sampled chamber and connect to the next one and still have enough time for the concentrations to reach a plateau before recording a time and concentration(s). There was roughly two minutes between chamber C and chamber A, this insured that each chamber was sampled every 5 minutes. This process is repeated for each hour. This method allows for the concentrations inside the chamber to increase for the remainder of the full hour.

For consistent and reliable measurement locations, a red buoy was installed and left at the deepest part of Uvas reservoir. During the monthly 24-hour sampling period, gas analyzer measurements were taken at the buoy as well as water quality measurements described in the next section.

3.2.3 In Situ measurements of water quality

Two Hydrolab DS5 sondes were deployed during each monthly 24-hour deployment to monitor water quality parameters. These ancillary measurements were taken to observe site climate and conditions at Uvas reservoir and to consider any relationships with the diffusive CO_2

concentrations at the air water interface. One sonde was placed in the shallow region, approximately ~2 meters from the water surface. The other sonde was placed in the deep end ~1-2 meters above the sediment bottom. Both sondes measured water quality parameters such as temperature in degrees Celsius (°C), pH, oxidation reduction potential in millivolts (mV) converted to 1 newton meter (nm), conductivity in micro-Siemens per centimeter (μS/cm), depth in meters (m), dissolved oxygen in milligrams per liter (mg/L), chlorophyll-a in microgram per liter (μg/L), converted to 1 newton meter (nm) at a 10-minute sampling rate. The two sondes were anchored to a buoy that was installed in the deepest part of the reservoir of the reservoir.

3.2.4 In Situ measurements of meteorological data

A meteorological station (MET station) was set up at the start of every monthly 24-hour deployment to collect data for observations and correlations with the flux rates of CO_2 at the air-water surface. The MET station set up included a steel tripod (CM106B), a main mast, and couple of crossarms used for the mounting of the atmospheric sensors (*Figure 3.2.1.3)*. It included the following sensors: an air temperature and relative humidity sensor (EE181-L) to measure the temperature of the air and relative humidity, a digital thermopile pyranometer (CS320) to measure incoming shortwave radiation, a barometric pressure sensor (CS106) to measure atmospheric pressure, and a wind monitor-HD (05108-L) to measure wind speed and direction. The sensors were powered by two 12V Power PS sonic rechargeable batteries and a 100-watt solar panel (Renology). It was important to align the wind monitor with respect to true North using a compass to identify the direction of the wind. The meteorological sensors were all hooked up to a Campbell scientific measurement and data logger (CR1000x). Atmospheric conditions were monitored during the surface gas sampling near the outlet of Uvas reservoir at a sampling rate of 1 minute.

Figure 3.2.3 MET station used throughout the 24-hour studies on Uvas Reservoir. The tower was attached with (a) an air temperature/relative humidity sensor, (b) a wind monitor, (c) a pyranometer, and (d) a Campbell Scientific measurement and data logger CR1000X with a barometer logger inside (e). The station was powered by two 12V Power PS Sonic rechargeable batteries and a 100-watt solar panel.

3.3 Quarterly Field Deployments

3.3.1 Field Sampling Sites

The quarterly sampling was conducted at three Santa Clara County Reservoirs: Uvas Reservoir, Chesbro Reservoir, and Steven's Creek Reservoir (*Figure 3.1.1*). The three reservoirs located in northern California each have their distinctive physical and bathymetric characteristics summarized in (*Table 3.3.1)*.

Table 3.3.1 Physical characteristic of each reservoir (Santa Clara County Parks n.d.)

Reservoir name	Max Storage Volume [m^3]	Max Surface Area [m^2]	Mean Depth [m]	Watershed [km^2]
Uvas	12,131,276	1,100,197	11.03	894.09
Chesbro	9,799,999	954,685	10.27	452.36
Stevens Creek	3,870,660	349,691	11.07	481.05

Uvas Reservoir (*37° 03' 56" N, 121° 41' 15" W*) was selected as the main site of interest for all the monthly field deployment sample collections because of its large size and water storage. Uvas Reservoir was constructed in 1957. It is an artificial mesotrophic lake located in the foothills of the Santa Cruz Mountains, CA (*Figure 3.3.1*). This lake is primarily used for ground water aquifer recharge and is used to pump into wells for residential, agricultural and industrial use (Santa Clara County Parks n.d.). Chesbro Reservoir (*37° 7'19.83"N, 121°42'23.76"W*) is also a mesotrophic lake that is smaller than Uvas and was constructed in 1955. The reservoir is surrounded by 232-acres which constitutes the Chesbro Reservoir County Park (*Figure 3.3.2*). The smallest of the three reservoirs in this study is Stevens Creek Reservoir (*37°17'45.91"N, 122° 4'39.29"W*). Stevens Creek was constructed in 1935 and resides in the center of the 1,063-acre Stevens Creek County Park (*Figure 3.3.3*).

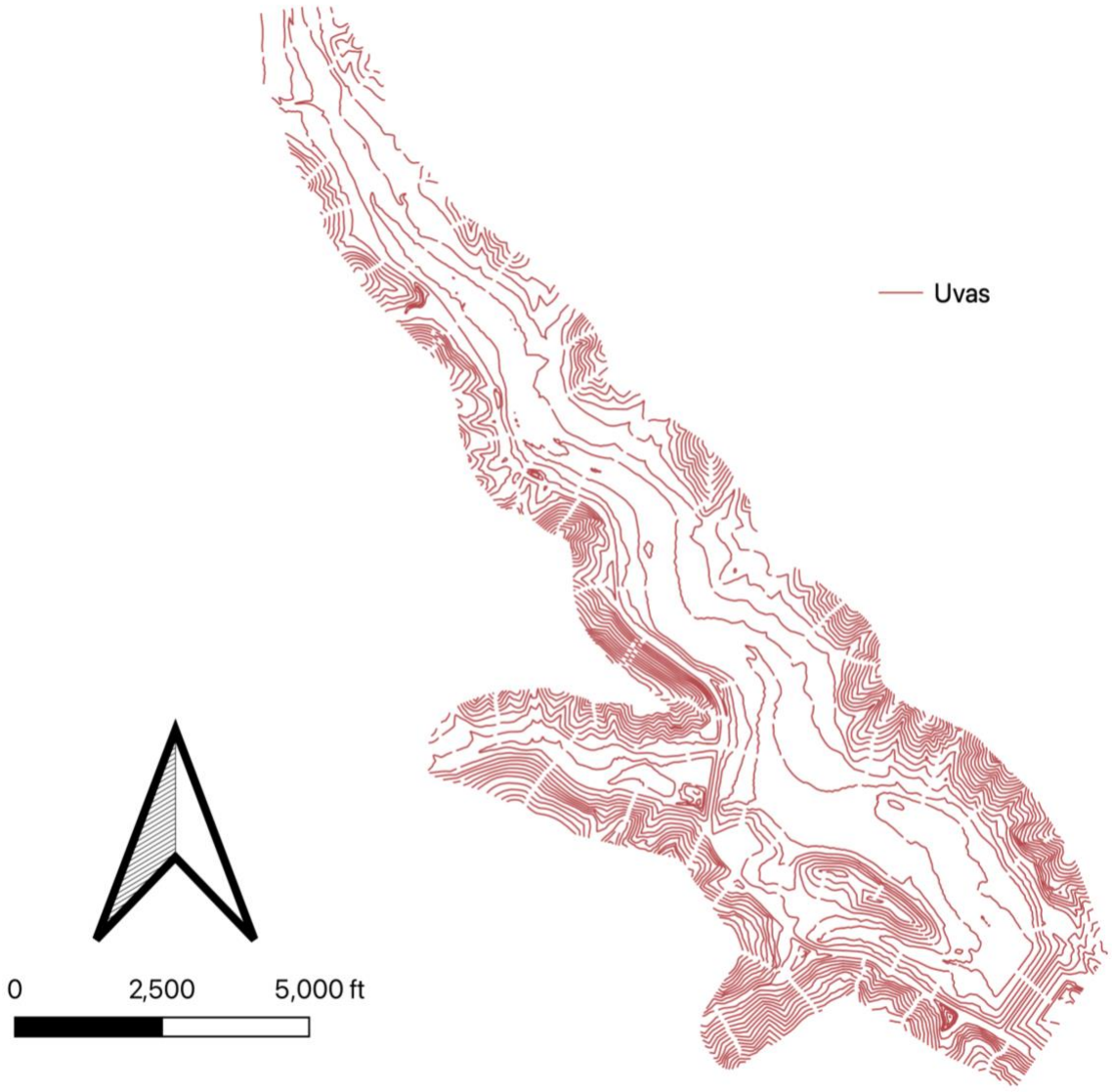

Figure 3.3.1 Uvas Reservoir is selected because it is the largest reservoir managed by Santa Clara County Valley Water.

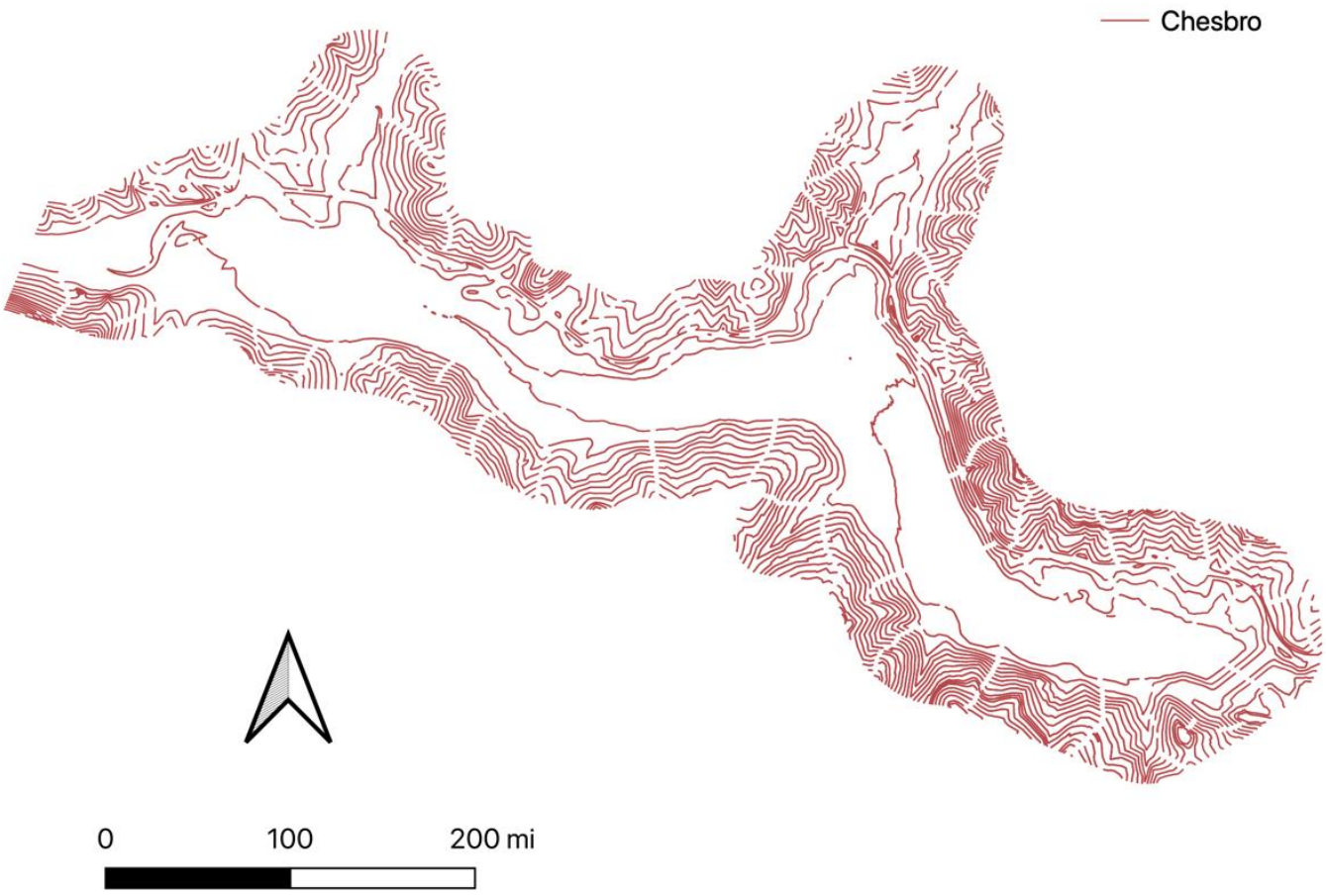

Figure 3.3.2 Chesbro Reservoir is located close to Uvas Reservoir and is also a mesotrophic lake.

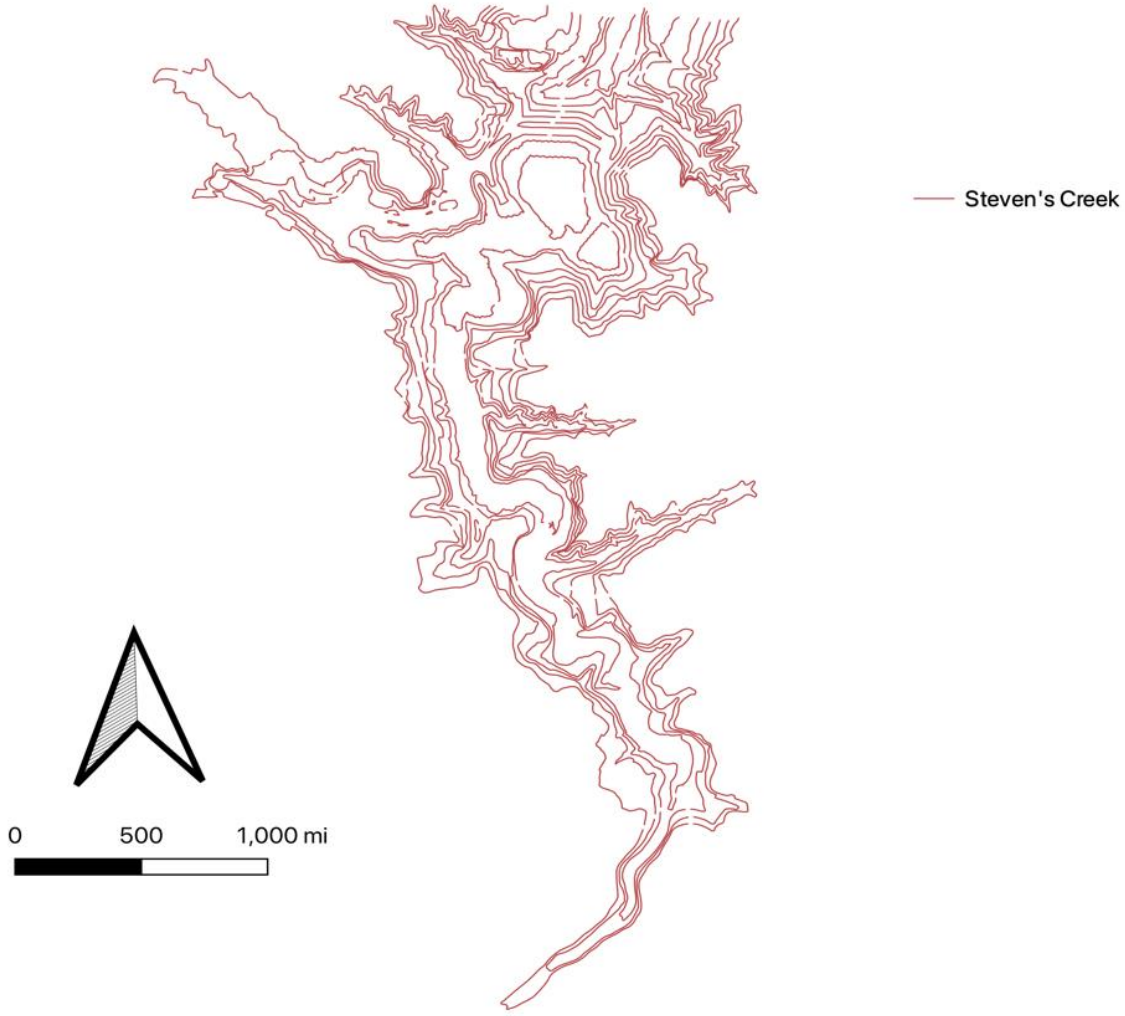

Figure 3.3.3 Stevens Creek Reservoir is a smaller and more productive lake compared to the other two study sites (see Section 4.3)

GPS Sampling Locations:

A significant segment of the project was to compare the differences between CO_2 diffusive fluxes from the water surface of these reservoirs. The sampling locations with GPS coordinates are presented below (*Figure 3.3.4*).

Stevens Creek Reservoir was sampled near the outlet (Latitude: 37°17’49.56”N, Longitude: 122° 4’39.00”W), in the middle (Latitude: 37°17’43.80”N, Longitude: 122° 4’34.32”W), and near the inlet (Latitude: 37°17’44.52”N, Longitude: 122° 4’46.92”W). Uvas Reservoir was sampled near the outlet (Latitude 37° 4’1.92”N, Longitude: 121°41’33.72”W), in the middle (Latitude: 37° 4’14.16”N, Longitude: 121°41’57.84”W), and near the inlet (Latitude: 37° 4’36.12”N, Longitude: 121°42’18.00”W).

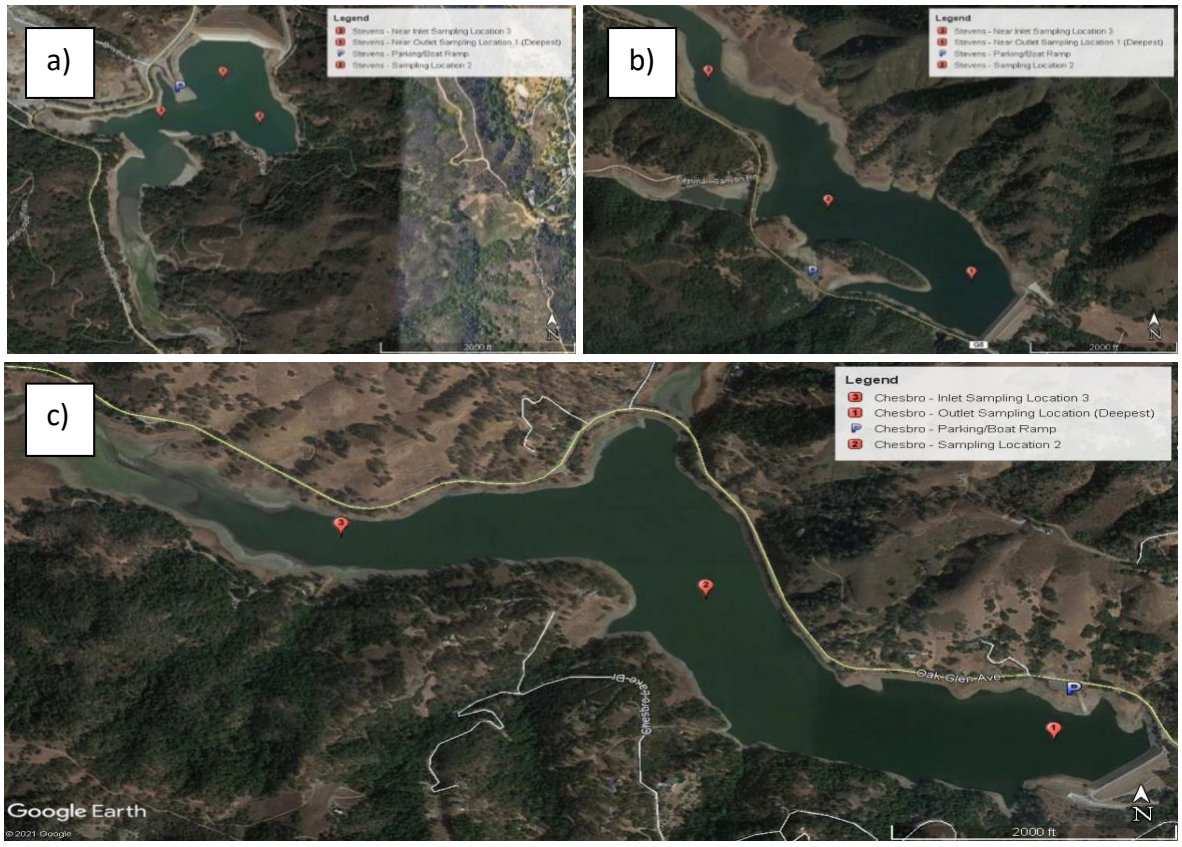

Figure 3.3.4 Quarterly sampling locations on a) Stevens Creek Reservoir, b) Uvas Reservoir, and c) Chesbro Reservoir. The red pins represent the sampling locations on each reservoir.

Chesbro Reservoir was sampled near the outlet (Latitude: 37° 7’1.20”N, Longitude: 121°41’45.60”W), in the middle (Latitude: 37° 7’15.24"N, Longitude: 121°42'15.84"W), and near the inlet (Latitude: 37° 7'21.36"N, Longitude: 121°42'47.52"W).

3.3.2 In Situ measurements of CO_2 surface fluxes

During all quarterly deployments, moorings were placed at the shallow, mid-depth, and deep sampling locations at least one hour before sampling to ensure that sediments were not disturbed at the time of sampling. Two members of the UC Davis research team would navigate to every sampling location and measure the surface GHG fluxes using an 8’ Zodiac with a 34-pound thrust trolling motor. Measurements of surface CO_2 concentrations were taken using the same procedure as described in the monthly 24-hour field sampling protocol.

3.3.3 In Situ measurements of water quality

Two Hydrolab DS5 sondes were deployed during every quarterly deployment to monitor water quality parameters and to observe any correlations with diffusive CO_2 flux rates at the air water interface. One sonde was placed near the outlet in the shallow region of the reservoir, approximately ~2 meters above the sediment bottom. The other sonde was placed in the deep region of the reservoir ~1-2 meters above the sediment bottom. Both sondes measured water quality parameters such as temperature in degrees Celsius (°C), pH, oxidation reduction potential recorded in millivolts (mV) and converted to newton meter (nm), conductivity in micro-Siemens per centimeter (μS/cm), depth in meters (m), dissolved oxygen in milligrams per liter (mg/L), chlorophyll-a in microgram per liter (μg/L), and phycocyanin in volts (V) converted to 1 newton meter (nm) at a 10-minute sampling rate. The two sondes were left in the water at each individual site throughout the entire sampling period.

3.4 Diffusive Flux Rate Calculations

Diffusive flux rates are calculated using the change in gas concentration inside the chamber over time, $\Delta c/\Delta t$, where Δc is the change in the areal gas flux [$mg \cdot m^{-2}$] (calculated from measured concentrations and Equation 14) and Δt is the change in time in minutes. At the beginning of each hourly sample, the three chambers were placed on surface of the water where the time was first recorded at zero minutes (as described in Section 3.3.2). For both the 24-hour and quarterly field deployments, the gas analyzer recorded raw data including date, time, gas concentrations, and gas temperature at a 5-second interval that was saved internally as a .txt file. The associated timestamp with each sample measured was stored in a format of *MM/dd/yyyy HH:mm:ss.SSS*. Gas concentrations collected from the gas analyzer were in units of ppm which were later converted to mg m^{-2} of CO_2 gas (*Equation 14).*

The following calculations using (*Equations 11 and 12),* use the ideal gas law to convert from gas concentrations of ppm to units of mg $\cdot$ m^{-3} through ideal gas law and unit conversion. The mole to volume ratio to parts per million by moles in air For CO_2:

$$1\ PPM\ CO_2 = \frac{1}{10^6}\left[\frac{mol\ CO_2}{mol\ air}\right] \cdot \frac{n}{V}\left[\frac{mol\ air}{L}\right] \cdot 44\left[\frac{g\ CO_2}{mol\ CO_2}\right] \cdot \frac{1000}{1}\left[\frac{mg}{g}\right] \cdot \frac{1000}{1}\left[\frac{L}{m^3}\right] \quad \text{(Equation 11)}$$

Converting grams to milligrams and liters to cubic meters cancels out the parts per million by moles of a given gas in the atmosphere.

$$1\ PPM\ CO_2 = \left[\frac{mol\ CO_2}{mol\ air}\right] \cdot \frac{n}{V}\left[\frac{mol\ air}{L}\right] \cdot 44\left[\frac{g\ CO_2}{mol\ CO_2}\right] \cdot \left[\frac{mg}{g}\right] \cdot \left[\frac{L}{m^3}\right]$$
$$= 44\ [\frac{mg\ CO_2}{m^3}]$$

(Equation 12)

Next, the temperature of the gas was taken from the gas analyzer output file labeled *GasT_C*. The gas temperature was stored in units of Celsius and was converted to temperature units of Kelvin by adding 273.15 to the output temperatures. Using the ideal gas law, the mole to volume was calculated assuming the atmospheric pressure, *P*, was equal to 1 atm and the universal gas constant, *R*, was equal to 0.0821 $\frac{L \cdot atm}{mol \cdot K}$. An example for typical atmospheric conditions is shown below *Equation 13*.

$$\frac{n}{v} = \frac{P}{RT} = \frac{1\ atm}{308.1795\ K\ * 0.0821 \frac{L * atm}{mol * K}} = 0.0395 \frac{\text{mol}}{L}$$

(Equation 13)

To calculate an aerial gas flux (i.e., mg · m^{-2}), the volumetric gas concentrations are multiplied by the volume of the chamber where the gas was collected and divided by the cross-sectional area of the chamber where the water surface was in contact with the chamber. An example CO_2 aerial flux calculation is shown below*:*

$$0.0395 \frac{\text{mol}}{L}\ * 44 \frac{g}{mol}\ * 401.4400 \frac{1\ mol\ gas}{10^6 mol\ air}\ * \frac{1\ mg}{10^{-3} g} * \frac{1L}{10^{-3} m^3}$$
$$= \frac{697.703 \frac{mg}{m^3} * 0.00891 m^3}{0.0423\ m^2} = 147 \frac{mg}{m^2}$$

(Equation 14)

Finally, to calculate a gas flux rate (i.e., mg · $m^{-2}h^{-1}$), each gas flux inside its respective chamber (A, B, and C) is then plotted against the differential time in minutes to create a relationship between aerial gas flux and time (for an example see *Figure 3.4.1)*.

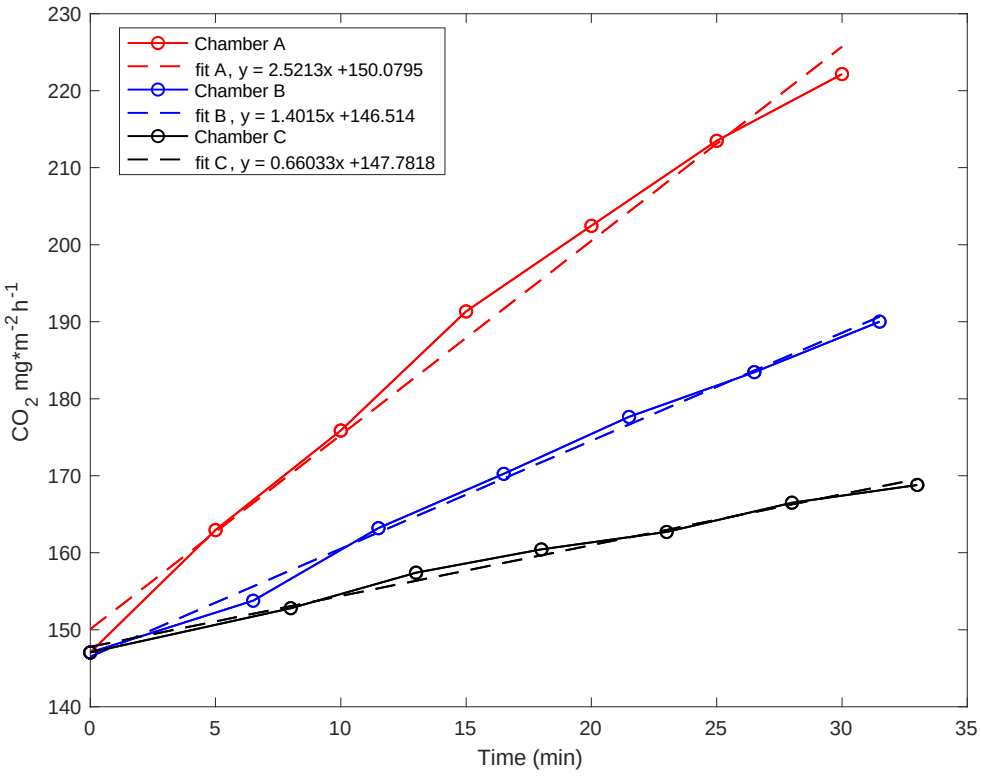

Figure 3.4.1 Depicting an example of how a temporal flux is calculated with respect to slope from Chamber A, slope for Chamber B, and slope from Chamber C. The average of all slopes is taken to find the diffusive flux of that hour.

The data points are used to plot the best fit line to find the slope within that hour (~60 mins). The slope of each trendline represents the diffusive flux rate from each chamber. The r-squared values help quantify the goodness of the linear fit. Resultingly, three diffusive chambers (chamber A, chamber B and chamber C) were used to measure the variability of diffusive fluxes at the surface waterline and all three were used to calculate an average diffusive flux and standard deviation for every hour sampled.

CHAPTER 4 RESULTS AND DISCUSSION

4.1 Carbon Dioxide Flux Measurement Results Overview

This chapter conveys the results of the study found by the CO_2 flux measurements taken from study sites (Uvas Reservoir, Chesbro Reservoir and Stevens Creek Reservoir) all located in a Mediterranean climate in the Santa Cruz mountains. First, the CO_2 flux results from the monthly 24-hour taken from Uvas Reservoir are presented to analyze the temporal (i.e., seasonal, and diel) variability and drivers, followed by the results from the quarterly taken from the three reservoirs Uvas, Chesbro and Stevens Creek to compare the spatial and seasonal variability. Lastly, the chapter will compare the CO_2 flux rates calculated from Uvas reservoir with other reservoirs located in different climatic regions and with CO_2 flux rates from different land cover types published from preceding literature.

4.2 Uvas Reservoir Temporal Variability

The water levels for sampling period of this study at Uvas Reservoir, 2021 were during California's second 'dry phase' period in a row during which drought conditions persisted. Stratified conditions of the water column occurred from the months of February through July and prohibited deep mixing in the reservoir. DO levels in the hypolimnion were very low from the months of March through September that corresponded to the stratification period (*Figure 4.2.1*). According to Fernández-González and Marañón (2021), the incident temperature for phytoplankton growth is at 18 ºC, whereas the optimal temperature for phytoplankton growth is at 25 ºC (Fernández-González and Marañón, 2021). In April at the beginning of the summer season, the water temperature was vertically stratified, and the surface water temperature became approximately 25°C. (*Figure 4.2.1*). The water temperature conditions allowed for uptake of CO_2 through gross primary production.

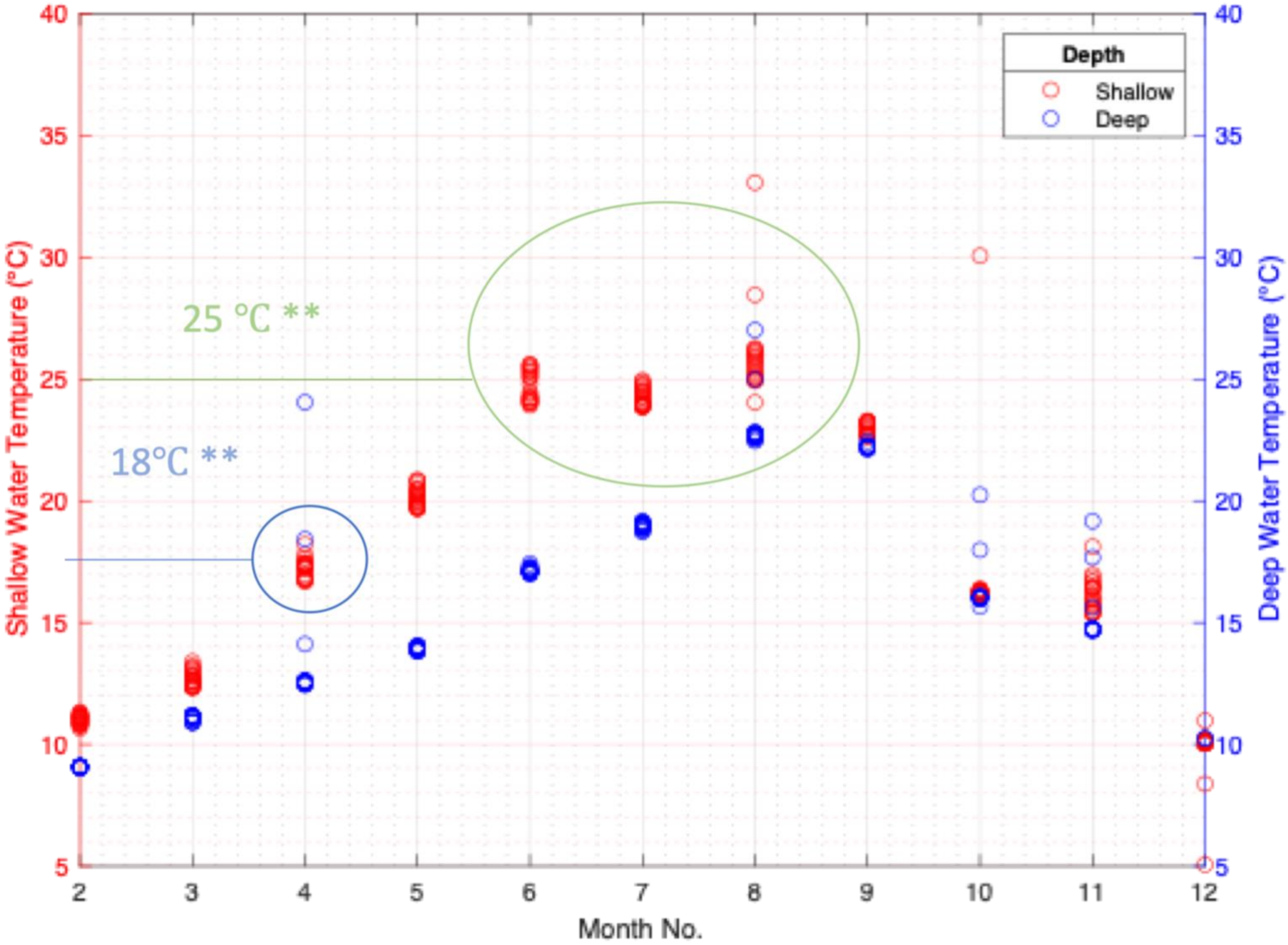

*Figure 4.2.1 Monthly temperature data for the shallow water (red, left axis) and deep water (blue, right axis) levels throughout the duration of the year. ** According to Fernández- González and Marañón 2021, the incident temperature for phytoplankton growth is at 18 ºC, whereas; the optimal temperature for phytoplankton growth is at 25ºC.*

Table 4.2.1 List of water quality parameters with recorded seasonal results from Uvas Reservoir.

PARAMETER	SEASON			
	Winter (Nov-Jan)	Spring (Feb - March)	Summer (Apr - Jul)	Fall (Aug- Oct)
WATER TEMPERATURE	Coolest	Warm	Warmest	Cool
SURFACE DO	Present	Present	Low	Present
DEEP DO	Present	Anoxic	Anoxic	Present
CHLOROPHYLL- A	Low	Highest	High	Lowest
CO_2 FLUX	Small source	High uptake	Low uptake	High source

The reservoir follows a seasonal pattern, where the forcings on the water are primarily generated by sunlight and wind which ultimately control the reservoir temperature temporally (*Figure 4.2.1*). The seasonal lake turnover takes place once in the fall and occurs when the temperature of the atmosphere cools the epilimnion resulting in the large density differences (thermocline) to vertically homogenize the three water column layers (i.e., epilimnion, metalimnion and hypolimnion). As a response to the destratification period along with turbulent mixing with air in the fall season at the air-water interface, DO is reintroduced into the hypolimnion. With such elevated levels of DO carrying over into the winter, this allows for ideal conditions for aerobic microbes to flourish. Along with DO, large amounts of nutrients are also impounded into the reservoir from allochthonous or autochthonous pathways throughout the winter season. Finally, once the reservoir hits the spring season there are plenty of nutrients and oxygen to support the metabolic processes. In February at the start of spring, there is high uptake of CO_2, or in simpler terms, the reservoir acts like a sponge and is a sink for CO_2 *(Figure 4.2.2)*.

The reservoir continues to remain a CO_2 sink throughout the spring up to mid-summer where the largest uptake occurs in June at -1.32 mg $\cdot$ $m^{-2}h^{-1}$. Once all the nutrients have been used up during photosynthesis, the reservoir undergoes diurnal alternations from a source during the day to a sink at night in the summer (*Figure 4.2.3*). This trend continues throughout the year with two critical high emission events that occur, one in the fall and the other in the winter. In September, the CO_2 fluxes spike to a maximum concentration value at 1.57 mg $\cdot$ m^{-2} h^{-1} in the daytime. In December, the CO_2 fluxes spike to a maximum concentration value at a value of 1.9 mg$\cdot$ m^{-2} h^{-1} in the daytime. After the fall turnover period in November, the water body becomes thermally stratified again and will remain stratified throughout the entire year as the lake is classified as a warm Monomictic system.

In November 2021, the shallow water reaches its peak chlorophyll-a concentration at a maximum of 100 μg $\cdot$ L^{-1} (*Figure 4.2.4*). The deep water, on the other hand, reaches a maximum of chlorophyll-a of 30 μg $\cdot$ L^{-1} in the same month. Significantly, the deeper layer of water in the stratified lake has a lower concentration of phytoplankton mass. This is because the hypolimnion lacks access to the solar radiation and photosynthetic bacteria, and as result, photosynthetic processes do not occur at theses lower depths. The seasonal and diel trends for CO_2 are apparent throughout the year, where CO_2 fluxes rates are positive in the fall months and in the nighttime. After the mixing period, the CO_2 and chlorophyll-a concentrations show homogeneity starting in February of 2021. The relationship between the flux rate of CO_2 and the surface chlorophyll-a concentration at Uvas Reservoir is relative to the seasonal changes (*Figure* 4.2.5). In the summer months (*Table 4.2.1)*, there is a negative correlation with CO_2 and surface chlorophyll-a. concentration This is a result of algae using up CO_2 through photosynthetic processes. Looking at the fall months, the results show a change from a negative to a positive relationship between

CO_2 and chlorophyll-a. This is depicted by both higher rates of CO_2 fluxes and chlorophyll-a. Uvas Reservoir is a mesotrophic reservoir, that is it has an intermediate level of productivity, which results in minimal output of CO_2 fluxes throughout the year.

In the spring and summer months when the water column is stratified, methanogenesis occurs under anaerobic conditions and produces CH_4 in the sediments but also in anoxic hypolimnia (Casper et al. 2000). Consequently, CH_4 oxidation (methanotrophy) occurs in the aerobic water column and results in CO_2 production and diffusion at the surface. More specifically, this phenomenon is also called methane stripping in which ultimately gives rise to an increase in CO_2 during these two seasonal periods of stratification. Throughout the entire year, Uvas Reservoir alternated between a CO_2 source and a sink. After summing all monthly flux rates, the total flux rate emitted for the year of 2021 is equivalent to + 21.17 $mg \cdot m^{-2}h^{-1}$. Thus, Uvas Reservoir is a net positive source of CO_2 to the atmosphere where Uvas Reservoir has positive values (CO_2 source) in the fall and winter, and negative values (CO_2 sink) in the summer and spring (*Figure 4.2.2*). The results are comparable to the findings from Montes-Pérez, et al. 2022, in which seasonal scale of temporal variability is considered in the study. However, it is also important to include an analysis on diurnal fluxes as our findings and those in Morales-Pineda et al. 2014, show that there is a relationship between environmental forcings and the different times scales throughout the day. For example, temperature is responsive to night cooling and convection, and light controls the balance between respiration and production.

The dataset presented in this thesis is unprecedented in its time resolution and show the important diel changes in CO_2 flux rates. The CO_2 flux rate observations in this study are important for obtaining global GHG estimates, as the results contribute to having a better understanding of temporal CO_2 flux rates from reservoirs located in a Mediterranean climate.

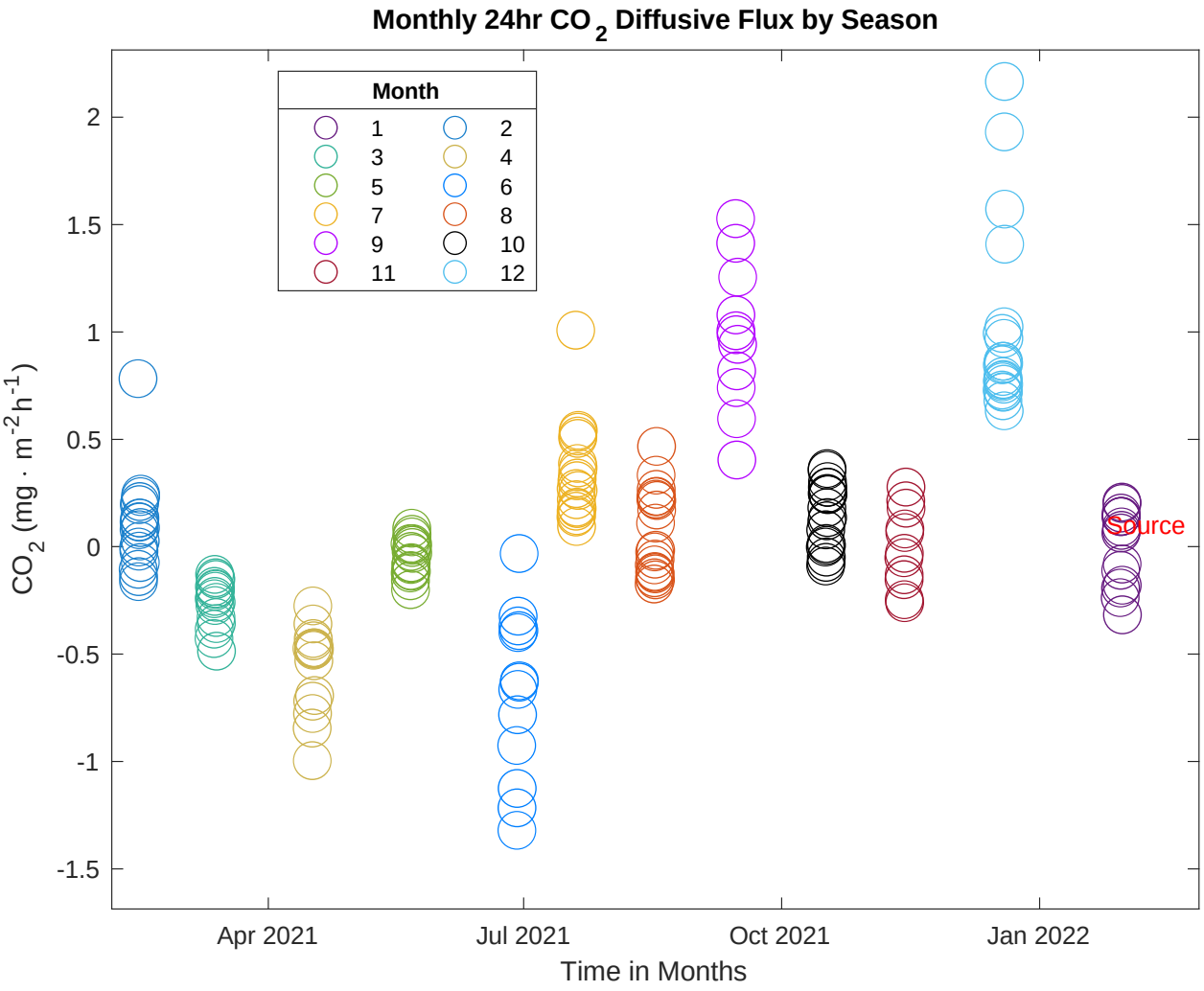

Figure 4.2.2 Represents all the CO_2 fluxes calculated throughout the full year of 2021.

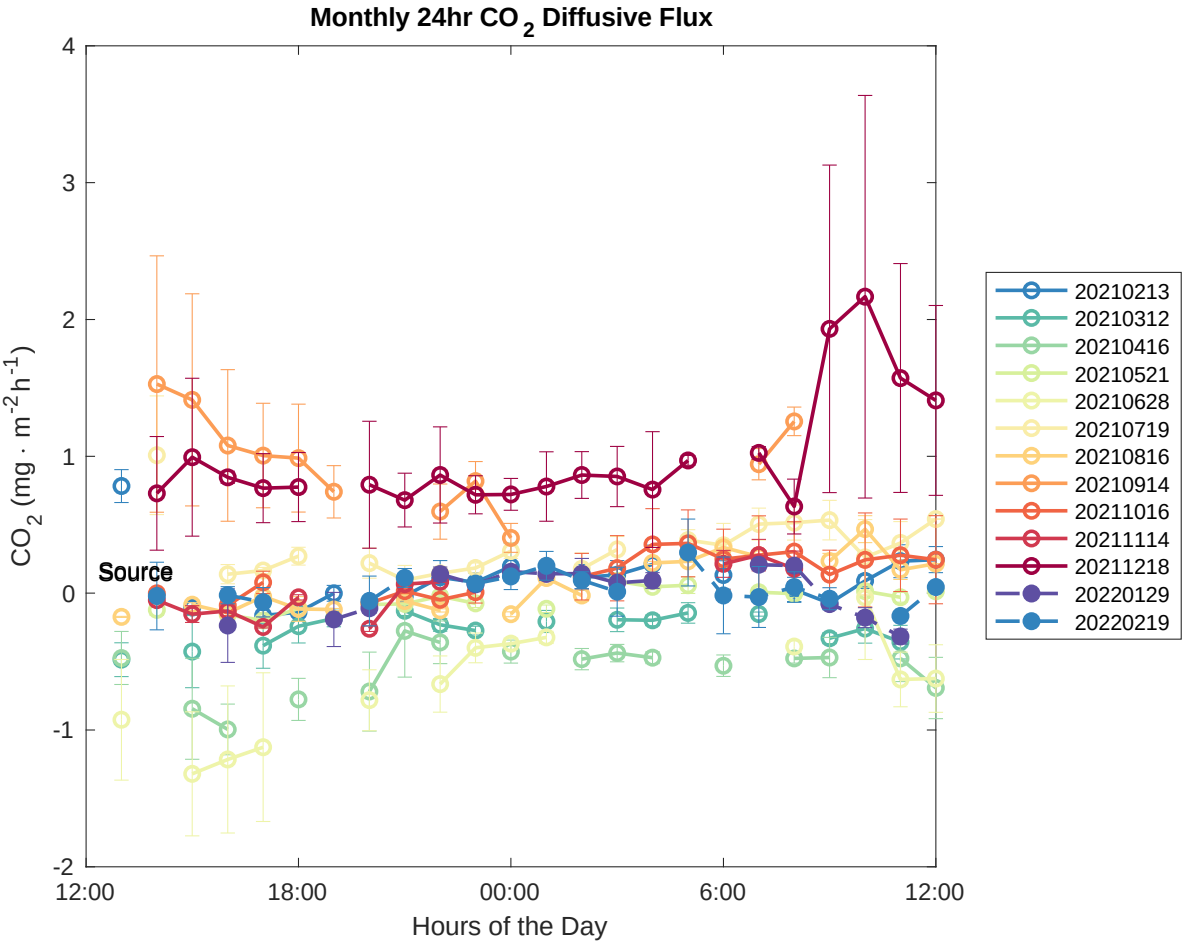

Figure 4.2.3 Represents the 24-hour CO_2 fluxes by hour taken each month. The error bars are representative of the standard deviation for each flux rate calculated.

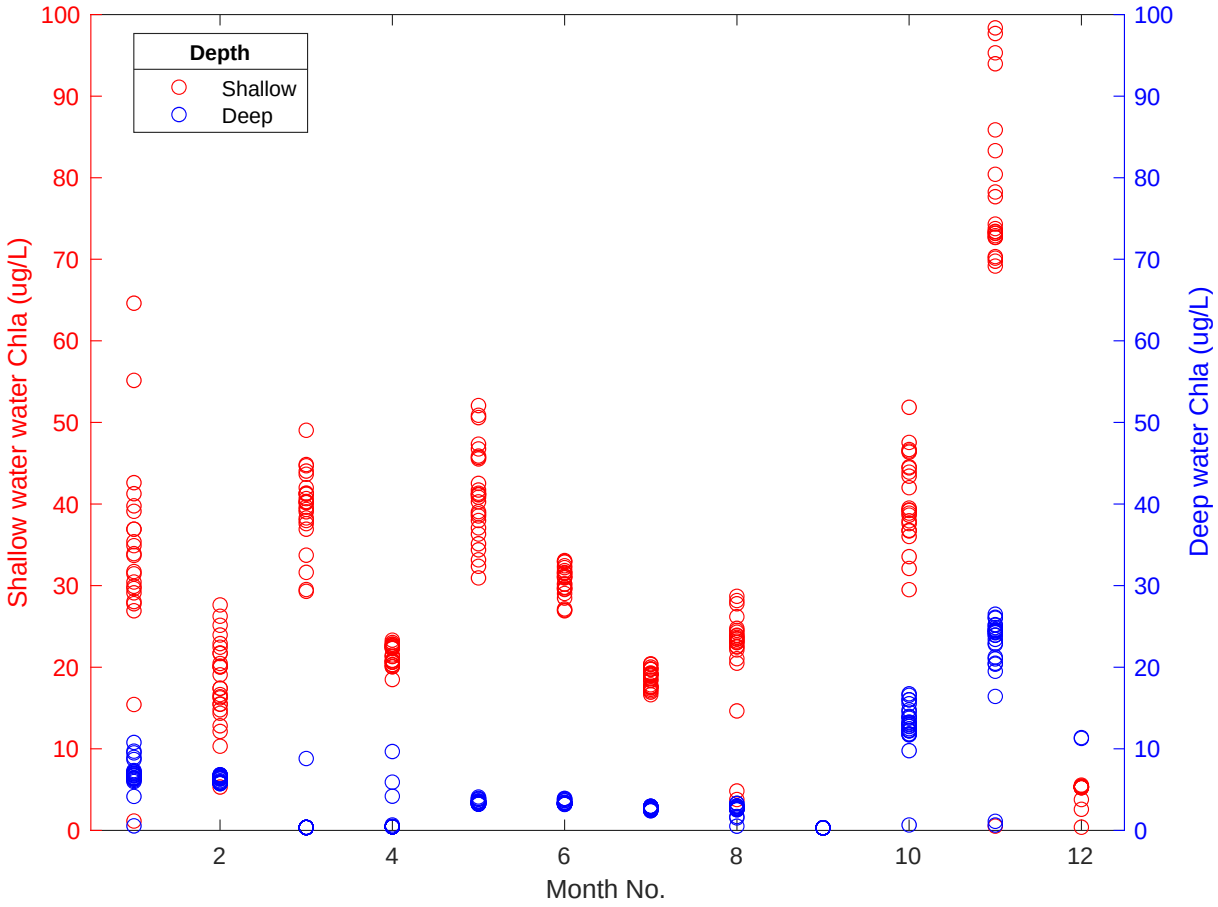

Figure 4.2.4 Monthly Chlorophyll-a data for the shallow water (red, left axis) and deep water (blue, right axis) levels throughout the duration of the year

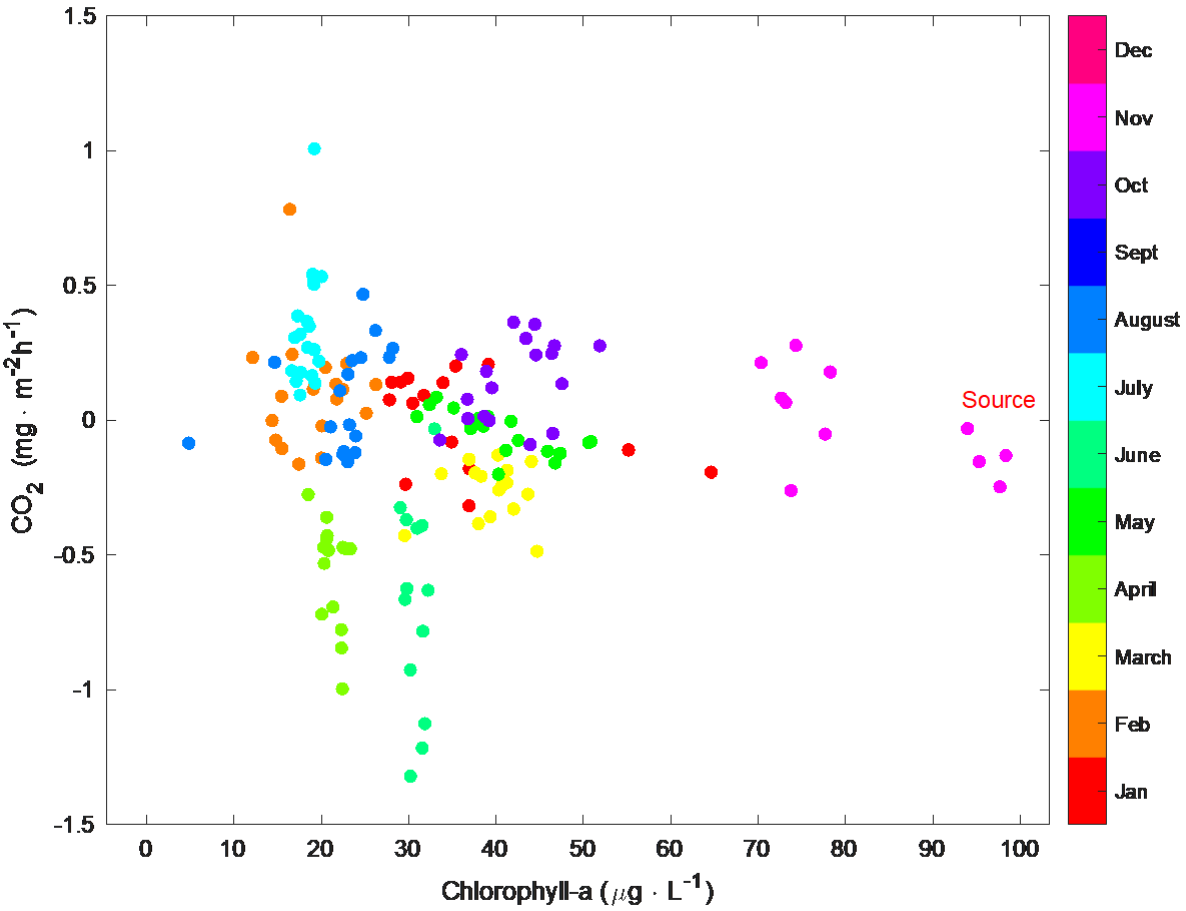

Figure 4.2.5 The relationship between CO_2 fluxes and Chl-a concentrations from the sonde placed at the shallow site for each month depicted by color.

4.3 Uvas, Chesbro, & Stevens Creek Reservoir Spatial Variability

The differences between CO_2 flux at the three reservoirs shows that the site at Chesbro Reservoir is the most productive compared to the other two reservoirs, as the reservoir experiences negative CO_2 flux rates throughout the fall, spring, and summer months and positive CO_2 flux rates in the winter *(Figure 4.3.1)*. The metabolic productive environment at Chesbro Reservoir results in a sink year-round until the winter. The reason Chesbro Reservoir is more productive year-round yet becomes a large sink in the winter compared to Uvas Reservoir, despite having a similar watershed, is likely because of its age. Chesbro Reservoir is the oldest site between the two reservoirs and shows that the soil organic matter, and decomposition of flooded material are sources of CO_2 fluxes. These findings are in line with previous studies that indicate the fluxes can remain significant for decades and even centuries due to the presence of large organic carbon storage present prior to flooding (Kelly et al. 1997; St. Louis et al. 2000; Venkiteswaran 2008). However, this idea is contrary to Barros et al., (2011) who propose that overtime, the emissions tend to decline with the age of the reservoir.

At Uvas Reservoir, the site is less productive and is a small source over the four seasons *(Figure 4.3.1)*. Interestingly, the reservoir surface water in the summer has little to no CO_2 efflux. In the winter season, Uvas reservoir's exhibits peak CO_2 emissions due to the reservoir turnover period reintroducing the nutrients and DO into the surface water and water column.

At Stevens Creek Reservoir, the reservoir remains a source of CO_2 throughout all seasons *(Figure 4.3.1)*. The specific conductivity measured at Stevens Creek Reservoir is the highest out of the three reservoirs and is characterized as the murkiest which indicates a higher number of impurities in the water (*Figure 4.3.2*). It was expected that because of the quality of the water, such as a higher conductivity, water temperature and pH, the reservoir would act as sink in the

summer, however; the results show otherwise. In the spring season at Uvas Reservoir and Chesbro Reservoir, prime CO_2 uptake (CO_2 sink) occurs because of essential replenishment and availability of plant nutrients. However, at Stevens Creek Reservoir, it instead reaches its largest flux output of CO_2 at ~1.8 $mg \cdot m^{-2} h^{-1}$. These unexpected results could be due to different factors. For one, the high turbidity and the low water levels influence and limit the DO and metabolic pathways of photosynthesis. Another factor to consider is that the lake was under heterotrophic conditions, that is when the rate of respiration is larger than the rate of gross primary production. The terrestrial organic carbon that may be exported to Stevens Creek Reservoir can increase lake heterotrophy.

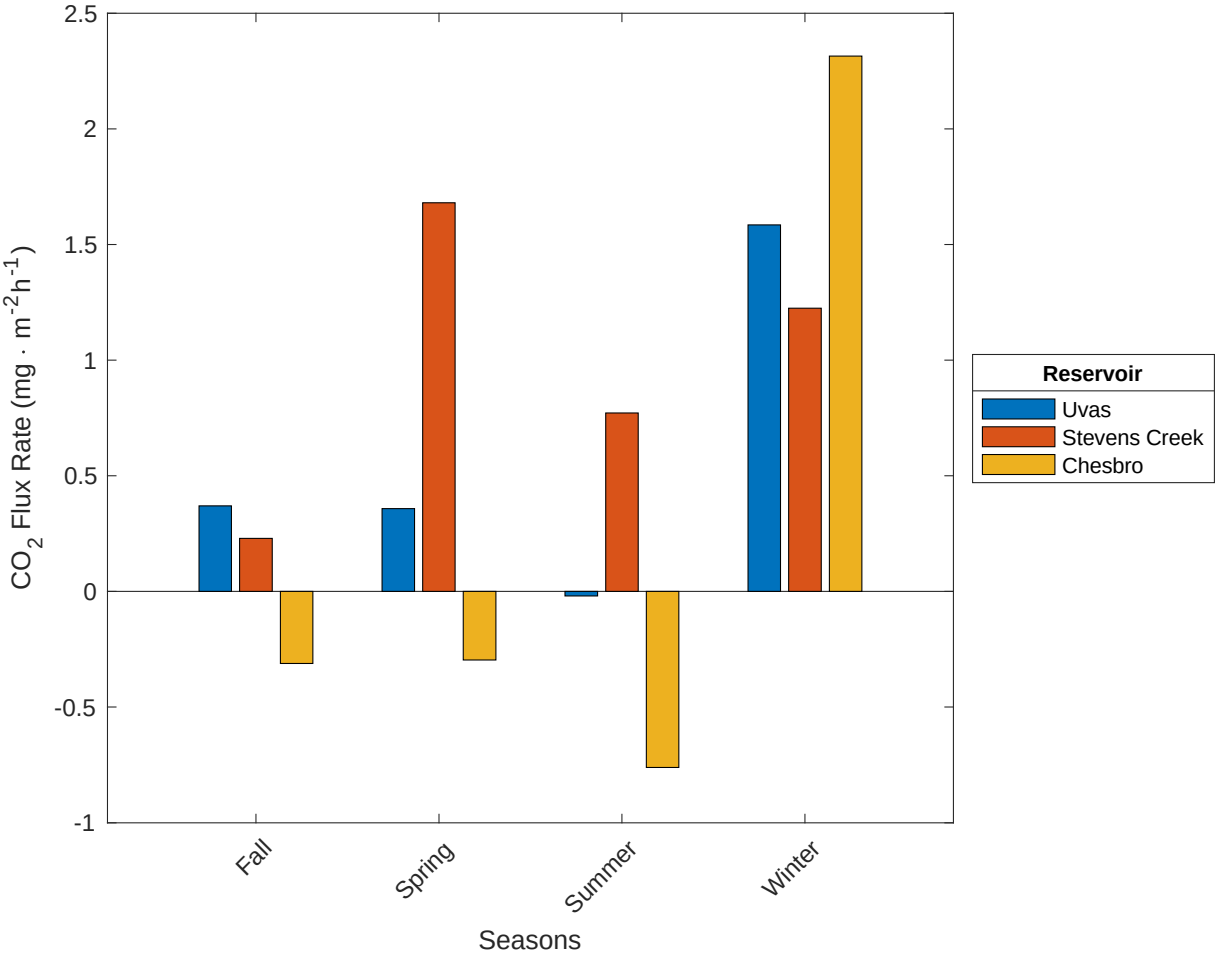

Figure 4.3.1 Seasonal CO_2 flux rates at all three reservoirs: Uvas, Stevens Creek, and Chesbro Reservoir throughout the 4 seasons in year 2021.

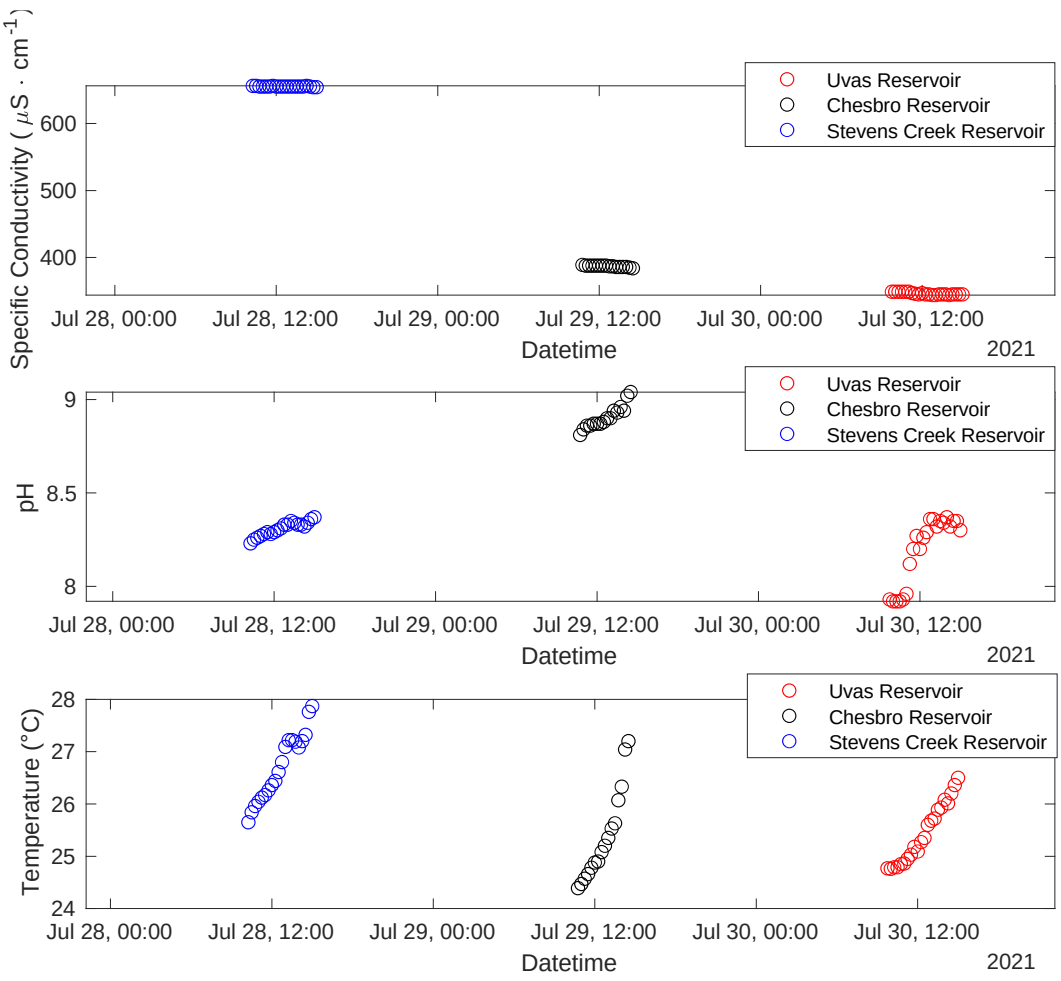

Figure 4.3.2 Surface water quality parameters from Uvas, Chesbro and Stevens Creek Reservoirs that indicate Stevens Creek had the highest specific conductivity and temperature under basic conditions. Data are specific to the summer quarterly which took place July 28, 2021 – July 30, 2021.

4.4 Climatic Region Impacts on Carbon Dioxide Fluxes

CO_2 flux rates vary spatially throughout the world's climatic regions (*Table 4.4.1)*. The total annual flux rate of +21.17 mg · $m^{-2}h^{-1}$ observed from Uvas Reservoir, located in a Mediterranean climate, show that there exists a substantial difference between reservoirs located in other climatic regions. In a Boreal climate, the annual average CO_2 flux emissions rate is found to be ~62.8 mg · $m^{-2}h^{-1}$ (Tremblay et al. 2005). In a Tropical climate, the annual average CO_2 flux emissions rate is found to be ~4.17 mg · $m^{-2}h^{-1}$ (Cardoso et al. 2013). For a Temperate climate, the annual average CO_2 flux emission rate is found to be approximately 1.31 mg · $m^{-2}h^{-1}$ (Knoll et al. 2013). Lastly, in a Polar climate, the annual CO_2 flux emission rate is found to be roughly 30.81 mg · $m^{-2}h^{-1}$ (Gerardo-Nieto et al. 2017). Previous literature and the present study indicate that across all climates, reservoirs can either result in large or small atmospheric CO_2 flux emissions annually and are not carbon zero systems.

Compared to Uvas Reservoir, Boreal and Polar regions have the highest mean annual CO_2 flux rates (*Figure 4.4.1) (*Tremblay et al., 2005 and Gerardo-Nieto et al., 2017). As previously mentioned, temperature has a crucial role in generating CO_2 gas fluxes. In colder climates, there is less sunlight throughout the year to drive photosynthetic processes resulting in larger CO_2 effluxes. In comparison, Uvas Reservoir has smaller flux rates than those in the Polar and Boreal regions but higher flux rates than those in tropical and temperate climatic regions where the weather is subjected to hotter and dryer conditions.

Although studies reveal that CO_2 gas flux rates vary across climatic regions, reservoirs from the same climate zone can differ from each other as well. For example, in the present study observing the Mediterranean climate at Uvas, Chesbro, and Stevens Creek Reservoir the results between the three sites have different flux rates. Therefore, future studies need to determine what

specific environmental forcings are drivers of CO_2 fluxes in its specific system and cannot base CO_2 flux rates on its climatic region location. The measurements of CO_2 flux rates in this study are important for obtaining both Mediterranean climate and global estimates where the results can give a better idea of the temporal variability of CO_2. Across diel and seasonal cycles, it is questionable whether CO_2 flux rates are released from every reservoir across all climatic regions. This calls for additional sampling deployments at different distinctive reservoirs that have not been studied, identify their CO_2 flux rates, and determine if they are net carbon zero or a net carbon emitter.

Table 4.4.1 Listing the four main climatic regions in across the world and their average CO_2 flux emission rates according to previous published literature. The values are taken from each reference stated in the table and converted to units of mg $\cdot m^{-2} h^{-1}$ for comparison in Figure 4.4 shown below.

CLIMATIC REGION	MEAN CO_2 FLUX RATES	MEAN CO_2 FLUX RATES CONVERTED TO MG $\cdot$ M^{-2} H^{-1}	REFERENCE
Boreal	1508 mg $\cdot$ m^{-2} d^{-1}	**62.83**	Tremblay et al., 2005
Tropical	100 mg $\cdot$ $m^{-2}d^{-1}$	**4.17**	Cardoso et al., 2013
Temperate	11.47 g $\cdot$ m^{-2} y^{-1}	**1.31**	Knoll et al., 2013
Polar	16.8 mmol $\cdot$ $m^{-2}d^{-1}$	**30.81**	Gerardo-Nieto et al., 2017

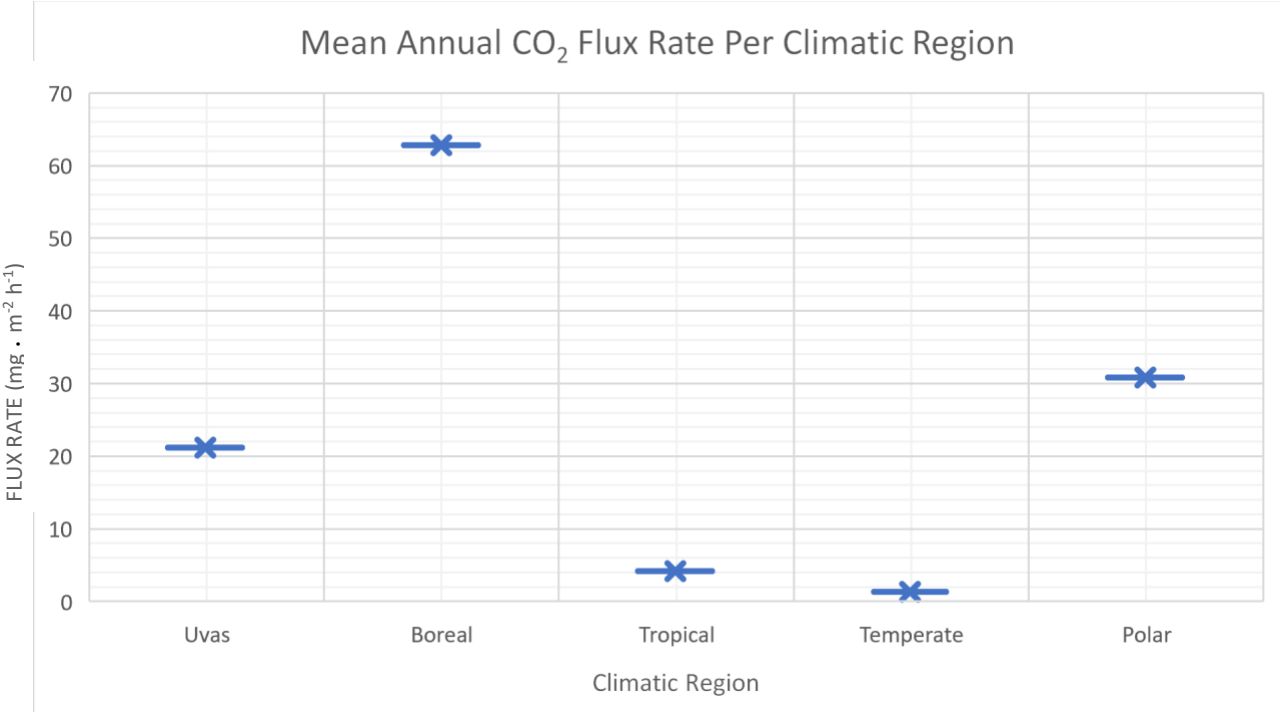

Figure 4.4.1 Different reservoirs from various climatic region gas flux rates compared to Uvas Reservoir.

4.5 Land Class Type Impacts on Carbon Dioxide Fluxes

Not only are CO_2 flux rates distinct across latitudes, but over different land class types as well (*Table 4.5.1).* Some major land classification types that influence the atmospheric gas fluxes include but are not limited to soils, streams, wetlands, peatlands, and the sea. Alongside inland waters, soil CO_2 fluxes are considered a dominant and significant regulator of climate change (Ma et al. 2013). The estimated mean CO_2 flux rate of soil ranges from 1.46 mg $\cdot$ $m^{-2}h^{-1}$ to 72.9 mg $\cdot$ $m^{-2}h^{-1}$ (Ma et al. 2013), given the limited data available. Streams have the most positive value with an average CO_2 flux rate of approximately 1321.2 mg $\cdot$ $m^{-2}h^{-1}$ (Billett and Harvey 2013). Streams are influenced by the high organic and inorganic carbon concentrations that result in heterotrophic conditions in these systems on an annual basis. Wetlands have an average CO_2 flux rate equivalent to –9.7 mg $\cdot$ $m^{-2}h^{-1}$ (Peter M. Lafleur, 2009). Peatlands are a type of wetland and are beneficial for mitigating the effects of climate change. On average, Peatlands have a CO_2 flux rate equivalent to 43.2 mg$\cdot$ m^{-2} h^{-1} (P. M. Lafleur et al. 2001). This is remarkable as Peatlands are supposed to mitigate the effects of climate change, instead they are contributing to CO_2 flux rates. The sea has an average CO_2 flux rate of 33 mg $\cdot$ m^{-2} h^{-1} (Bates and Merlivat 2001).

Uvas Reservoir has a mean annual flux of 21.17 mg $\cdot$ $m^{-2}h^{-1}$. There is a sizeable difference between the land classification type where streams and rivers have the highest flux rates of CO_2 (*Figure 4.5.1).* Conversely, wetlands are known to be advantageous and are CO_2 sinks where the microbial photosynthesis dominates the system and balances the CO_2 emissions (Machado et al. 2007).

Table 4.5.1 Listing the main land classification types across the globe that mediate CO_2 transfer into the atmosphere with its associated reference by author and year.

LAND CLASS TYPE	MEAN CO_2 FLUX RATE	MEAN CO_2 FLUX RATE CONVERTED TO MG · M^{-2} H^{-1}	REFERENCE
Soil	35.0-1749.4 mg · $m^{-2}d^{-1}$	**72.9**	Ma et al., 2013
Streams	367 μg · $m^{-2}s^{-1}$	**1321.2**	Billet and Harvey, 2013
Wetlands	-85 g · $m^{-2}y^{-1}$	**9.70**	Lafleur, 2009
Peatlands	0.012 mg · $m^{-2}s^{-1}$	**43.2**	Lafleur et al., 2001
Sea	$3.3 \cdot 10^{-2}$ g · m^{-2} h^{-1}	**33**	Bates and Merlivat, 2001

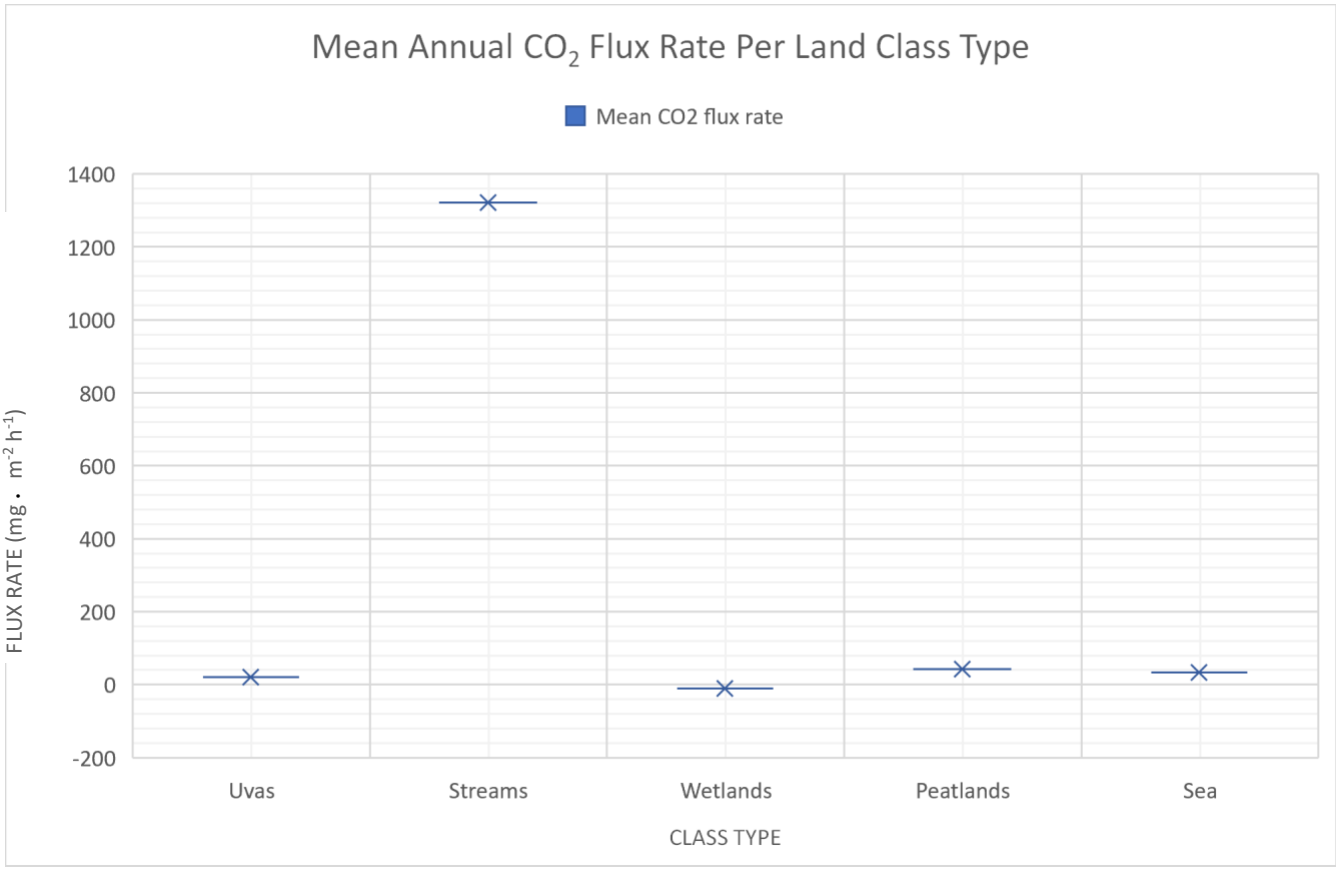

Figure 4.5.1 Land classification types mean annual CO_2 flux rates compared to Uvas Reservoir.

CHAPTER 5 CONCLUSIONS AND RECOMMENDATIONS

5.1 Summary of Study

The overall objective of this thesis was to use the floating chamber method to measure CO_2 flux rates from Uvas Reservoir to determine if the reservoir was a net source of carbon emissions. Uvas Reservoir was sampled every month to compare the temporal variability over one day (24-hours). The study also included an additional two reservoirs Stevens Creek and Chesbro Reservoirs to compare the spatial differences.

The research findings from this study show that even though the reservoirs Uvas Reservoir and Chesbro Reservoir are a part of the same watershed, Uvas/Llagas Watershed where 3 cities are shared and linked, Chesbro Reservoir experiences a significant CO_2 sink year-round. However, in the winter months the reservoir will be saturated in CO_2 causing the reservoir to shift from a sink to having the largest flux rate at ~2.45 $mg*m^{-2}*h^{-1}$. Chesbro Reservoir is the oldest and most productive, this could be a consequence of the reservoir's overall water quality.

Uvas Reservoir, the main site of interest exhibited complete CO_2 saturation where the reservoir was filled with CO_2 in the fall and winter months after the fall overturn. The reservoir CO_2 flux rates show a significant relationship with chlorophyll-a as expected, where there is a negative slope in the summer showing that as CO_2 decreases, chlorophyll-a increases and positive slope in the fall showing that as CO_2 increases, chlorophyll-a increases. The biological characteristics have a big of a role on the CO_2 surface gas fluxes. For further exploration, the physical dynamics in the air to water interface should be studied to identify if surface gas fluxes are dictated by physical forcings. This can be done by taking microstructure profiles of the reservoir, which is taken by a microstructure profiler instrument that measures the shear velocity temperature variability on vertical scales. A microstructure profile can analyze more frequent

wind patterns along with an increase of CO_2 gas flux rate measurements. Measuring the water tells us about the turbulent dissipation rates which is important when estimated CO_2 flux rate.

Stevens Creek is a part of the Lower Peninsula Watershed, where 6 cities share and transport runoff to. Stevens Creek is both the oldest and smallest reservoir between the other two reservoir sites in this study. The reservoir is subjected to murky water conditions, but because of its shallowness and desiccation periods it acts as a source throughout all the four seasons.

Aquatic ecosystem conditions are undergoing alterations that affect the physical and biological processes because of climate change. Longer, and/or permanent stratification periods could dominate reservoirs worldwide. This threatens GHG emissions as longer stratification periods lead to anaerobic digestion which can increase the process of other metabolic processes, producing substantial GHGs from other sources like methane. The study concludes that Uvas Reservoir follows the trends of previous literature and is a sink for CO_2 in the spring and summer but acts as a source for CO_2 in the fall and winter. However, under a changing climate carbon metabolism is suspected to alter the CO_2 flux rates (Tranvik et al. 2009) where hydrology and changing temperature will magnify the intensity of carbon cycling – burial and outgassing of carbon.

5.2 Future Work and Recommendations

The year 2021 was California's second consecutive extreme dry year (California Department of Water Resources, 2021), and Uvas Reservoir succumbed to being a reservoir GHG source in the fall and winter months. For future work, a study on the wet season is needed for further analysis of Mediterranean reservoirs to see the role that precipitation, runoff, nutrient loading, cloudy skies, and high-water storage have on CO_2 gas flux.

Wind is another important factor that influences gas transfer at the air-water interface. To gain more accurate representations of CO_2 temporal and spatial fluxes, implementing more direct measurements is advised. Therefore, with the eddy covariance technique, there would be greater spatial data to account for the wind speed and variability of the fluxes. In addition to the installation of the eddy covariance, there should be more frequent sampling with the floating chamber methods. For additional data collection, more fieldwork deployments are essential. The methods should be revised to include more frequent data sampling periods within the year. The current data is based on one day out of the month and is not representative of the full month, which might show higher CO_2 flux rate averages.

In addition to more frequent sampling periods, more gas flux chambers should be constructed for greater variability and precision. Having more gas flux chambers out in the field would be ideal because if one chamber gets lost, leaks, or becomes unreliable, then the data will be untrustworthy. Thus, losing one chamber would not have such a large impact on the field data and cause erroneous inferences.

As the climate warms up, the hydrological cycle will be affected, leading to fewer but also more intense periods of rainfall. In dry climates like California, it is important to plan for and create adaptation strategies that will mitigate the substantial impacts of drought. Creating a larger groundwater storage infrastructure will promote recharge when surface water flows become excessively in demand. This will create climate resilience during extended periods of drought. Another strategy for practicing climate resilience is increasing water storage capacity by either raising dams, removing accumulated sediment in reservoirs, or both. Implementing green infrastructure can have major benefits and is one way to enhance climate resilience. Green infrastructure is cost-effective and can provide sites for habitation, flood protection, cleaner

energy, and cleaner air (IPCC, 2012). Climate-smart cities can use green infrastructure to save energy by absorbing stormwater and recharging aquifers. Examples of stormwater management practices include the implementation of green roofs, rain barrels and cisterns, permeable pavements, bioretention areas, and constructed wetlands (EPA, 2022). Additionally, in urban cities and environments, the urban heat island effect can also be mitigated by implementing green spaces and providing shade to areas that heat up quickly and radiate heat fluxes back into the atmosphere.

Air temperatures, water temperatures, and larger amounts of nutrients in freshwater bodies due to storm runoff are increasing. These conditions threaten the quality of the reservoir by generating harmful algal blooms. Risk management practices use rainwater and storm runoff as resources instead of threats. This could be done by allocating specific flooding spaces and storage capacities. By reducing and controlling the runoff amounts, stormwater runoff can be better managed, and the quality of the runoff improved. More research would help to understand and identify the different approaches that engineering, and management could implement to reduce CO_2 fluxes from Mediterranean climate zones.

CHAPTER 6 REFERENCES

Anderson, Michael A., and Denise Martinez. 2015. "Methane Gas in Lake Bottom Sediments Quantified Using Acoustic Backscatter Strength." *Journal of Soils and Sediments* 15 (5): 1246–55. https://doi.org/10.1007/s11368-015-1099-1.

Arblaster, J, G Brasseur, J H Christensen, K L Denman, D W Fahey, P Forster, E Jansen, et al. 2007. "Climate Change 2007: The Physical Science Basis: Summary for Policymakers.," February.

Bastviken, David, Jonathan Cole, Michael Pace, and Lars Tranvik. 2004. "Methane Emissions from Lakes: Dependence of Lake Characteristics, Two Regional Assessments, and a Global Estimate." *Global Biogeochemical Cycles* 18 (4). https://doi.org/10.1029/2004GB002238.

Bates, Nicholas R., and Liliane Merlivat. 2001. "The Influence of Short-Term Wind Variability on Air-Sea CO2 Exchange." *Geophysical Research Letters* 28 (17): 3281–84. https://doi.org/10.1029/2001GL012897.

Billett, M. F., and F. H. Harvey. 2013. "Measurements of CO2 and CH4 Evasion from UK Peatland Headwater Streams." *Biogeochemistry* 114 (1): 165–81. https://doi.org/10.1007/s10533-012-9798-9.

Brown, Terry-René W., Marc J. Lajeunesse, and Kathleen M. Scott. 2020. "Strong Effects of Elevated CO2 on Freshwater Microalgae and Ecosystem Chemistry." *Limnology and Oceanography* 65 (2): 304–13. https://doi.org/10.1002/lno.11298.

Brutsaert, W., and G. H. Jirka. 2013. *Gas Transfer at Water Surfaces*. Springer Science & Business Media.

Butman, D., R. Striegl, S. Stackpoole, P. del Giorgio, Y. Prairie, D. Pilcher, P. Raymond, et al. 2018. "Chapter 14: Inland Waters. Second State of the Carbon Cycle Report." U.S. Global Change Research Program. https://doi.org/10.7930/SOCCR2.2018.Ch14.

California Department of Water Resources. 2021. "Water Year 2021: An Extreme Year," September.

Campbell-Lendrum, Diarmid, Carlos Corvalán, and Maria Neira. 2007. "Global Climate Change: Implications for International Public Health Policy." *Bulletin of the World Health Organization* 85 (3): 235–37. https://doi.org/10.2471/BLT.06.039503.

Cardoso, Simone, Luciana Vidal, Raquel Mendonça, Lars Tranvik, Sebastian Sobek, and Fabio Roland. 2013. "Spatial Variation of Sediment Mineralization Supports Differential CO2 Emissions from a Tropical Hydroelectric Reservoir." *Frontiers in Microbiology* 4. https://www.frontiersin.org/articles/10.3389/fmicb.2013.00101.

Casper, Peter, Stephen C. Maberly, Grahame H. Hall, and Bland J. Finlay. 2000. "Fluxes of Methane and Carbon Dioxide from a Small Productive Lake to the Atmosphere." *Biogeochemistry* 49 (1): 1–19. https://doi.org/10.1023/A:1006269900174.

Chu, Housen, Xiangzhong Luo, Zutao Ouyang, W. Stephen Chan, Sigrid Dengel, Sébastien C. Biraud, Margaret S. Torn, et al. 2021. "Representativeness of Eddy-Covariance Flux Footprints for Areas Surrounding AmeriFlux Sites." *Agricultural and Forest Meteorology* 301–302 (May): 108350. https://doi.org/10.1016/j.agrformet.2021.108350.

Cole, J. J., Y. T. Prairie, N. F. Caraco, W. H. McDowell, L. J. Tranvik, R. G. Striegl, C. M. Duarte, et al. 2007. "Plumbing the Global Carbon Cycle: Integrating Inland Waters into the Terrestrial Carbon Budget." *Ecosystems* 10 (1): 172–85. https://doi.org/10.1007/s10021-006-9013-8.

Cole, Jonathan J., and Nina F. Caraco. 1998. “Atmospheric Exchange of Carbon Dioxide in a Low-Wind Oligotrophic Lake Measured by the Addition of SF6.” *Limnology and Oceanography* 43 (4): 647–56. https://doi.org/10.4319/lo.1998.43.4.0647.

Cole, Jonathan J., Nina F. Caraco, George W. Kling, and Timothy K. Kratz. 1994. “Carbon Dioxide Supersaturation in the Surface Waters of Lakes.” *Science* 265 (5178): 1568–70.

Czikowsky, Matthew J., Sally MacIntyre, Edmund W. Tedford, Javier Vidal, and Scott D. Miller. 2018. “Effects of Wind and Buoyancy on Carbon Dioxide Distribution and Air-Water Flux of a Stratified Temperate Lake.” *Journal of Geophysical Research: Biogeosciences* 123 (8): 2305–22. https://doi.org/10.1029/2017JG004209.

Deemer, Bridget R., John A. Harrison, Siyue Li, Jake J. Beaulieu, Tonya DelSontro, Nathan Barros, José F. Bezerra-Neto, Stephen M. Powers, Marco A. dos Santos, and J. Arie Vonk. 2016. “Greenhouse Gas Emissions from Reservoir Water Surfaces: A New Global Synthesis.” *BioScience* 66 (11): 949–64. https://doi.org/10.1093/biosci/biw117.

Delsontro, T., D.F. McGinnis, B. Wehrli, and I. Ostrovsky. 2015. “Size Does Matter: Importance of Large Bubbles and Small-Scale Hot Spots for Methane Transport.” *Environmental Science and Technology* 49 (3): 1268–76. https://doi.org/10.1021/es5054286.

Deshmukh, C., D. Serça, C. Delon, R. Tardif, M. Demarty, C. Jarnot, Y. Meyerfeld, et al. 2014. “Physical Controls on CH_4 Emissions from a Newly Flooded Subtropical Freshwater Hydroelectric Reservoir: Nam Theun 2.” *Biogeosciences* 11 (15): 4251–69. https://doi.org/10.5194/bg-11-4251-2014.

Eugster, Werner, George Kling, Tobias Jonas, Joseph P. McFadden, Alfred Wüest, Sally MacIntyre, and F. Stuart Chapin III. 2003. “CO2 Exchange between Air and Water in an Arctic Alaskan and Midlatitude Swiss Lake: Importance of Convective Mixing.” *Journal of Geophysical Research: Atmospheres* 108 (D12). https://doi.org/10.1029/2002JD002653.

Fafard, Paul. 2018. “How and Why Lakes Stratify and Turn Over: We Explain the Science behind the Phenomena – IISD Experimental Lakes Area.” May 16, 2018. https://www.iisd.org/ela/blog/commentary/lakes-stratify-turn-explain-science-behind-phenomena/.

Fernández-González, Cristina, and Emilio Marañón. 2021. “Effect of Temperature on the Unimodal Size Scaling of Phytoplankton Growth.” *Scientific Reports* 11 (1): 953. https://doi.org/10.1038/s41598-020-79616-0.

Gerardo-Nieto, Oscar, María Soledad Astorga-España, Andrés Mansilla, and Frederic Thalasso. 2017. “Initial Report on Methane and Carbon Dioxide Emission Dynamics from Sub-Antarctic Freshwater Ecosystems: A Seasonal Study of a Lake and a Reservoir.” *Science of The Total Environment* 593–594 (September): 144–54. https://doi.org/10.1016/j.scitotenv.2017.02.144.

Graziano, Giuseppe. 2014. “Hydrostatic Pressure Effect on Hydrophobic Hydration and Pairwise Hydrophobic Interaction of Methane.” *The Journal of Chemical Physics* 140 (9): 094503. https://doi.org/10.1063/1.4866972.

Haines, A, RS Kovats, D Campbell-Lendrum, and C Corvalan. 2006. “Climate Change and Human Health: Impacts, Vulnerability, and Mitigation.” *The Lancet* 367 (9528): 2101–9. https://doi.org/10.1016/S0140-6736(06)68933-2.

Haines, Andy, Anthony J McMichael, Kirk R Smith, Ian Roberts, James Woodcock, Anil Markandya, Ben G Armstrong, et al. 2009. “Public Health Benefits of Strategies to

Reduce Greenhouse-Gas Emissions: Overview and Implications for Policy Makers." *The Lancet* 374 (9707): 2104–14. https://doi.org/10.1016/S0140-6736(09)61759-1.
Horne, Alexander J., and Charles Remington Goldman. 1994. *Limnology*. 2nd ed. New York: McGraw-Hill.
Huang, Juping, Weiyang Zhao, Zhe Li, Yangming Ou, and Lu Lin. 2022. "Estimation of CO2 Emission in Reservoir Coupling Floating Chamber and Thin Boundary Layer Methods." *Science of The Total Environment* 811 (March): 151438. https://doi.org/10.1016/j.scitotenv.2021.151438.
Keller, P. S., N. Catalán, D. von Schiller, H.-P. Grossart, M. Koschorreck, B. Obrador, M. A. Frassl, et al. 2020. "Global CO2 Emissions from Dry Inland Waters Share Common Drivers across Ecosystems." *Nature Communications* 11 (1): 2126. https://doi.org/10.1038/s41467-020-15929-y.
Kelly, C. A., J. W. M. Rudd, R. A. Bodaly, N. P. Roulet, V. L. St.Louis, A. Heyes, T. R. Moore, et al. 1997. "Increases in Fluxes of Greenhouse Gases and Methyl Mercury Following Flooding of an Experimental Reservoir." *Environmental Science & Technology* 31 (5): 1334–44. https://doi.org/10.1021/es9604931.
Knoll, Lesley B., Michael J. Vanni, William H. Renwick, Elizabeth K. Dittman, and Jessica A. Gephart. 2013. "Temperate Reservoirs Are Large Carbon Sinks and Small CO2 Sources: Results from High-Resolution Carbon Budgets." *Global Biogeochemical Cycles* 27 (1): 52–64. https://doi.org/10.1002/gbc.20020.
Kosten, Sarian, Fábio Roland, David M. L. Da Motta Marques, Egbert H. Van Nes, Néstor Mazzeo, Leonel da S. L. Sternberg, Marten Scheffer, and Jon J. Cole. 2010. "Climate-Dependent CO2 Emissions from Lakes." *Global Biogeochemical Cycles* 24 (2). https://doi.org/10.1029/2009GB003618.
Kotcher, John, Edward Maibach, Jeni Miller, Eryn Campbell, Lujain Alqodmani, Marina Maiero, and Arthur Wyns. 2021. "Views of Health Professionals on Climate Change and Health: A Multinational Survey Study." *The Lancet Planetary Health* 5 (5): e316–23. https://doi.org/10.1016/S2542-5196(21)00053-X.
Lafleur, P. M., N. T. Roulet, and S. W. Admiral. 2001. "Annual Cycle of CO2 Exchange at a Bog Peatland." *Journal of Geophysical Research: Atmospheres* 106 (D3): 3071–81. https://doi.org/10.1029/2000JD900588.
Lafleur, Peter M. 2009. "Connecting Atmosphere and Wetland: Trace Gas Exchange." *Geography Compass* 3 (2): 560–85. https://doi.org/10.1111/j.1749-8198.2008.00212.x.
Levy, Barry, and Jonathan Patz. 2015. *Climate Change and Public Health*. Oxford University Press.
Li, Yi, Jiahui Shang, Chi Zhang, Wenlong Zhang, Lihua Niu, Longfei Wang, and Huanjun Zhang. 2021. "The Role of Freshwater Eutrophication in Greenhouse Gas Emissions: A Review." *Science of The Total Environment* 768 (May): 144582. https://doi.org/10.1016/j.scitotenv.2020.144582.
Lindsey, Rebecca. 2017. "How El Niño and La Niña affect the winter jet stream and U.S. climate | NOAA Climate.gov." September 18, 2017. http://www.climate.gov/news-features/featured-images/how-el-ni%C3%B1o-and-la-ni%C3%B1a-affect-winter-jet-stream-and-us-climate.
"Climate Change: Atmospheric Carbon Dioxide | NOAA Climate.gov." June 23, 2022. http://www.climate.gov/news-features/understanding-climate/climate-change-atmospheric-carbon-dioxide.

Lionello, Piero, Fatima Abrantes, Letizia Congedi, Francois Dulac, Miro Gacic, Damià Gomis, Clare Goodess, et al. 2012. “Introduction: Mediterranean Climate—Background Information.” In *The Climate of the Mediterranean Region*, edited by Piero Lionello, xxxv–xc. Oxford: Elsevier. https://doi.org/10.1016/B978-0-12-416042-2.00012-4.

Liu, Heping, Qianyu Zhang, Gabriel G. Katul, Jonathan J. Cole, F. Stuart Chapin, and Sally MacIntyre. 2016. “Large CO2 Effluxes at Night and during Synoptic Weather Events Significantly Contribute to CO2 Emissions from a Reservoir.” *Environmental Research Letters* 11 (6): 064001. https://doi.org/10.1088/1748-9326/11/6/064001.

López, Pilar, Rafael Marcé, and Joan Armengol. 2011. “Net Heterotrophy and CO2 Evasion from a Productive Calcareous Reservoir: Adding Complexity to the Metabolism-CO2 Evasion Issue.” *Journal of Geophysical Research: Biogeosciences* 116 (G2). https://doi.org/10.1029/2010JG001614.

Ma, Jie, Zhong-Yuan Wang, Bryan A. Stevenson, Xin-Jun Zheng, and Yan Li. 2013. “An Inorganic CO2 Diffusion and Dissolution Process Explains Negative CO2 Fluxes in Saline/Alkaline Soils.” *Scientific Reports* 3 (1): 2025. https://doi.org/10.1038/srep02025.

Machado, A.P., L. Urbano, A.G. Brito, P. Janknecht, J.J. Salas, and R. Nogueira. 2007. “Life Cycle Assessment of Wastewater Treatment Options for Small and Decentralized Communities.” *Water Science and Technology* 56 (3): 15–22. https://doi.org/10.2166/wst.2007.497.

Macintyre, Sally, Werner Eugster, and George Kling. 2002. “MacIntyre, S. W. Eugster, and G.W. Kling. 2001. The Critical Importance of Buoyancy Flux for Gas Flux Across,” March.

MacIntyre, Sally, and John M. Melack. 1995. “Vertical and Horizontal Transport in Lakes: Linking Littoral, Benthic, and Pelagic Habitats.” *Journal of the North American Benthological Society* 14 (4): 599–615. https://doi.org/10.2307/1467544.

Mackay, Donald, and Wan Ying Shiu. 1984. “Physical-Chemical Phenomena and Molecular Properties.” In *Gas Transfer at Water Surfaces*, edited by Wilfried Brutsaert and Gerhard H. Jirka, 3–16. Water Science and Technology Library. Dordrecht: Springer Netherlands. https://doi.org/10.1007/978-94-017-1660-4_1.

McDowell, Mollie Jean. 2017. “Determining Gas Transfer Velocitites and CO2 Evasion Fluxes from Streams Using Carbon Dioxide as a Tracer,” August. https://open.library.ubc.ca/media/stream/pdf/24/1.0355223/3.

McGinnis, Daniel F., Georgiy Kirillin, Kam W. Tang, Sabine Flury, Pascal Bodmer, Christof Engelhardt, Peter Casper, and Hans-Peter Grossart. 2015. “Enhancing Surface Methane Fluxes from an Oligotrophic Lake: Exploring the Microbubble Hypothesis.” *Environmental Science & Technology* 49 (2): 873–80. https://doi.org/10.1021/es503385d.

Minear, J. Toby, and G. Matt Kondolf. 2009. “Estimating Reservoir Sedimentation Rates at Large Spatial and Temporal Scales: A Case Study of California: TECHNICAL NOTE.” *Water Resources Research* 45 (12). https://doi.org/10.1029/2007WR006703.

Montes-Pérez, J. J., R. Marcé, B. Obrador, T. Conejo-Orosa, J. L. Díez, C. Escot, I. Reyes, and E. Moreno-Ostos. 2022. “Hydrology Influences Carbon Flux through Metabolic Pathways in the Hypolimnion of a Mediterranean Reservoir.” *Aquatic Sciences* 84 (3): 36. https://doi.org/10.1007/s00027-022-00867-2.

Montes-Pérez, J. J., B. Obrador, T. Conejo-Orosa, V. Rodríguez, R. Marcé, C. Escot, I. Reyes, J. J. Rodríguez, and E. Moreno-Ostos. 2022. “Spatio-Temporal Variability of Carbon

Dioxide and Methane Emissions from a Mediterranean Reservoir." *Limnetica* 41 (1): 43–60. https://doi.org/10.23818/limn.41.04.

Morales-Pineda, María, Andrés Cózar, Irene Laiz, Bárbara Úbeda, and José Á. Gálvez. 2014. "Daily, Biweekly, and Seasonal Temporal Scales of PCO2 Variability in Two Stratified Mediterranean Reservoirs." *Journal of Geophysical Research: Biogeosciences* 119 (4): 509–20. https://doi.org/10.1002/2013JG002317.

NOAA. 2022. "Greenhouse Gas Pollution Trapped 49% More Heat in 2021 than in 1990, NOAA Finds - Welcome to NOAA Research." May 23, 2022. https://research.noaa.gov/article/ArtMID/587/ArticleID/2877/Greenhouse-gas-pollution-trapped-49-more-heat-in-2021-than-in-1990-NOAA-finds.

Park, Hyungseok, and Sewoong Chung. 2018. "PCO2 Dynamics of Stratified Reservoir in Temperate Zone and CO2 Pulse Emissions During Turnover Events." *Water* 10 (10): 1347. https://doi.org/10.3390/w10101347.

Park, Hyungseok, Sewoong Chung, and Sungjin Kim. 2021. "Effect of Buoyant Turbulence and Water Quality Factors on the CO2 Net Atmospheric Flux Changes in a Stratified Reservoir." *Science of The Total Environment* 776 (July): 145940. https://doi.org/10.1016/j.scitotenv.2021.145940.

Podgrajsek, E., E. Sahlée, D. Bastviken, J. Holst, A. Lindroth, L. Tranvik, and A. Rutgersson. 2014. "Comparison of Floating Chamber and Eddy Covariance Measurements of Lake Greenhouse Gas Fluxes." *Biogeosciences* 11 (15): 4225–33. https://doi.org/10.5194/bg-11-4225-2014.

Raymond, Peter A., Jens Hartmann, Ronny Lauerwald, Sebastian Sobek, Cory McDonald, Mark Hoover, David Butman, et al. 2013. "Global Carbon Dioxide Emissions from Inland Waters." *Nature* 503 (7476): 355–59. https://doi.org/10.1038/nature12760.

Rocha, João, Cláudia Carvalho-Santos, Paulo Diogo, Pedro Beça, Jan Jacob Keizer, and João Pedro Nunes. 2020. "Impacts of Climate Change on Reservoir Water Availability, Quality and Irrigation Needs in a Water Scarce Mediterranean Region (Southern Portugal)." *Science of The Total Environment* 736 (September): 139477. https://doi.org/10.1016/j.scitotenv.2020.139477.

Santa Clara County Parks. n.d. "Uvas Reservoir County Park - Parks and Recreation - County of Santa Clara." Accessed February 15, 2023. https://parks.sccgov.org/santa-clara-county-parks/uvas-reservoir-county-park.

Smith, S. V. 1985. "Physical, Chemical and Biological Characteristics* of CO2 Gas Flux across the Air-Water Interface." *Plant, Cell & Environment* 8 (6): 387–98. https://doi.org/10.1111/j.1365-3040.1985.tb01674.x.

St. Louis, V.L., C.A. Kelly, É. Duchemin, J.W.M. Rudd, and D.M. Rosenberg. 2000. "Reservoir Surfaces as Sources of Greenhouse Gases to the Atmosphere: A Global Estimate." *BioScience* 50 (9): 766–75. https://doi.org/10.1641/0006-3568(2000)050[0766:RSASOG]2.0.CO;2.

Tranvik, Lars J., John A. Downing, James B. Cotner, Steven A. Loiselle, Robert G. Striegl, Thomas J. Ballatore, Peter Dillon, et al. 2009. "Lakes and Reservoirs as Regulators of Carbon Cycling and Climate." *Limnology and Oceanography* 54 (6part2): 2298–2314. https://doi.org/10.4319/lo.2009.54.6_part_2.2298.

Tremblay, Alain, Jean Therrien, Bill Hamlin, Eva Wichmann, and Lawrence J. LeDrew. 2005. "GHG Emissions from Boreal Reservoirs and Natural Aquatic Ecosystems." In *Greenhouse Gas Emissions — Fluxes and Processes: Hydroelectric Reservoirs and*

Natural Environments, edited by Alain Tremblay, Louis Varfalvy, Charlotte Roehm, and Michelle Garneau, 209–32. Environmental Science. Berlin, Heidelberg: Springer. https://doi.org/10.1007/978-3-540-26643-3_9.

Vachon, Dominic, Yves T. Prairie, and Jonathan J. Cole. 2010. "The Relationship between Near-Surface Turbulence and Gas Transfer Velocity in Freshwater Systems and Its Implications for Floating Chamber Measurements of Gas Exchange." *Limnology and Oceanography* 55 (4): 1723–32. https://doi.org/10.4319/lo.2010.55.4.1723.

Venkiteswaran, Jason James. 2008. "Greenhouse Gas Cycling in Experimental Boreal Reservoirs."

Waldo, Sarah, Jake J. Beaulieu, William Barnett, D. Adam Balz, Michael J. Vanni, Tanner Williamson, and John T. Walker. 2021. "Temporal Trends in Methane Emissions from a Small Eutrophic Reservoir: The Key Role of a Spring Burst." *Biogeosciences* 18 (19): 5291–5311. https://doi.org/10.5194/bg-18-5291-2021.

Wetzel, ROBERT G. 2001. "11 - THE INORGANIC CARBON COMPLEX." In *Limnology (Third Edition)*, edited by ROBERT G. Wetzel, 187–204. San Diego: Academic Press. https://doi.org/10.1016/B978-0-08-057439-4.50015-0.

Zappa, Christopher J., Wade R. McGillis, Peter A. Raymond, James B. Edson, Eric J. Hintsa, Hendrik J. Zemmelink, John W. H. Dacey, and David T. Ho. 2007. "Environmental Turbulent Mixing Controls on Air-Water Gas Exchange in Marine and Aquatic Systems." *Geophysical Research Letters* 34 (10). https://doi.org/10.1029/2006GL028790.

Zhao, Yan, Bradford Sherman, Phillip Ford, Maud Demarty, Tonya DelSontro, Atle Harby, Alain Tremblay, et al. 2015. "A Comparison of Methods for the Measurement of CO_2 and CH_4 Emissions from Surface Water Reservoirs: Results from an International Workshop Held at Three Gorges Dam, June 2012: Intercomparison of GHG Measurements." *Limnology and Oceanography: Methods* 13 (1): 15–29. https://doi.org/10.1002/lom3.10003.